Experimental Analysis of a Hybrid Thermal Storage Wall – Water Heating System

Marzieh Rezaei

Submitted to the
Institute of Graduate Studies and Research
in partial fulfillment of the requirements for the degree of

Master of Science
in
Mechanical Engineering

Eastern Mediterranean University
August 2015
Gazimağusa, North Cyprus

Approval of the Institute of Graduate Studies and Research

Prof. Dr. Serhan Çiftçioğlu
Acting Director

I certify that this thesis satisfies the requirements as a thesis for the degree of Master of Science in Mechanical Engineering.

Prof. Dr. Uğur Atikol
Chair, Department of Mechanical Engineering

We certify that we have read this thesis and that in our opinion it is fully adequate in scope and quality as a thesis for the degree of Master of Science in Mechanical Engineering.

Prof. Dr. Uğur Atikol
Supervisor

Examining Committee

1. Prof. Dr. Uğur Atikol
2. Prof. Dr. Fuat Egelioğlu
3. Dr. Davut Solyali

ABSTRACT

The aim of this study is to evaluate the performance of the thermal storage wall (TSW) of the Solar Energy Research, Inspection and Training (SolERIT) laboratory in the Eastern Mediterranean University. The laboratory building has a floor area of 10 m^2 and the walls are not insulated. The façade of TSW facing to south has an area of 8.037m^2. An array of piping was fastened on the outer surface of the TSW to form a solar collector for heating water that can be used in heating applications of the rooms normally located in the northern parts of the buildings. Recording of solar radiation and temperatures of the ambient, TSW and water flow through the pipes were conducted during selected days of March 2015.

It was found that the temperature and solar radiation variations during the day influence the performance of the TSW. TSW performed well specially on sunny days with 9-15 $^{\circ}$C temperature drops at nights. Cyprus is a suitable area for taking advantage of TSW during winter.

The results of experiments showed that with the TSW under test the lowest room temperature in the coldest day (i.e. 12th March) was 17 $^{\circ}$C while the ambient temperature was 7 $^{\circ}$C. It was observed that the water pipes fixed on TSW surface played an important role on the efficiency of hybrid TSW – water heating system and low-grade heat could be accumulated in a tank for utilizing in other heating applications.

Keywords: Thermal storage wall, Trombe wall, solar collector, solar energy laboratory, North Cyprus

ÖZ

Gün boyunca sıcaklık ve güneş radyasyonu varyasyonları termal depolama duvarının performansını etkileyebilir. Isıl depolama duvarının (IDD) güneşli iklimlerde ve günlük sıcaklık dalgalanmalarında olumlu bir performans göstermesi bekleniyor. Kıbrıs, kışın IDD'nin avantajlarından yararlanmak için uygun bir bölgede yer almaktadır.

Bu çalışmanın amacı, Doğu Akdeniz Üniversitesi Güneş Enerjisi Araştırma, Denetleme ve Eğitim (SolERIT) Laboratuvarında bulunan IDD'nin performansını değerlendirmektir. Laboratuvar binası, 10 m^2 taban alanına sahip ve duvarlar izolasyonlu değildir. IDD'nin güneye bakan cephesi 8.037m^2 bir alana sahiptir. güneş kolektörü oluşturmak için boru dizisi IDD'nin dış yüzeyinde tespit edildi. Bu sistem suyu ısıtmada kullanılabilir ve odaların ısıtma uygulamalarında normalde binaların kuzey bölgelerine monte edilir. Güneşin ışınımı ve IDD ile kollektöre su giriş çıkışı sıcaklıkları Mart 2015'in seçilen günlerinde kayıt altına alınmıştır.

Deneylerin sonuçları, 8,073 m2 alana sahip bir IDD'nın en soğuk günde (12 Mart), ortam sıcaklığının 7 ^{o}C olduğu bir sırada oda sıcaklığı 17 ^{o}C olarak ölçülmüştür. IDD yüzeyinin üzerine sabitlenen su boruları IDD ve su ısıtma sistemlerinin perfomansinda çok önemli rolü vardır ve tankın içersinde toplanan düşük derecedeki ısı miktarları diğer ısıtma sistemlerinde kullanılabilir.

Anahtar kelimeler: Isıl depolama duvarı, Trombe duvarı, güneş kolektörü, güneş enerjisi laboratuvarı, Kuzey Kıbrıs

ACKNOWLEDGMENT

Firstly, I would like to express my sincere gratitude to my advisor Prof.Dr. Uğur Atikol for the continuous support of my master study and related research, for his patience, motivation, and immense knowledge. His guidance helped me in all the time of research and writing of this thesis. I could not have imagined having a better advisor and mentor for my master study.

My sincere thanks also go to Dr. Maher Ghazal who share with me his knowledge about laboratory and his research experience. Without his precious support it would not be possible to conduct this thesis.

Last but not the least; I would like to thank my parents for supporting me spiritually throughout writing this thesis.

TABLE OF CONTENTS

LIST OF TABLES

LIST OF FIGURES

LIST OF SYMBOLS

TSW	Thermal storage wall
PV	Photovoltaic
SolERIT	Solar Energy Research Inspection and Training
K	Kelvine
Q	heat
$\dot{m}$	Rate of mass
C_p	Specific heat capacity
Nu	Nusselt number
Ra_L	Rayleigh number
Gr_L	Grashof number
Pr	Prandtl number
g	Gravitational accelerative
ν	Dynamic viscosity
L	Length of TSW
k	Thermal conductivity
A_s	Heat transfer area

h	Heat transfer coefficient
T_f	Film temperature
S	Solar radiation
T	Temperature

Subscripts

a	Ambient
tw	Thermal wall
r	Room
w,in	Inlet water
w,out	Outlet water

Greek symbol

η	Efficiency
ρ	Density

Chapter 1

INTRODUCTION

There has been a growth in the world's population and a parallel increase in energy demand in the last decades. In addition, due to the lack of fossil fuels in some countries, scientists have been researching on alternative methods for energy conservation especially in residential usage, since these accounts for a major part of energy consumption.

Cyprus is an island which suffers from lack of natural oil resources. Before electricity was adopted, wood was the only type of fuel produced, and also the only heating source. Due to increases in energy demand and changes in buildings style, Cypriots prefer to use electric energy instead of wood. Therefore, high cost of imported fuel forced the consumers to consider alternative sources. On the other hand, energy efficiency is hardly practiced in North Cyprus. As a result, high energy demand and absence of energy sources is the reason for seeking alternative energy sources in Cyprus.

The use of solar energy technologies can be a feasible alternative to using of fossil fuels. Amongst available solar technologies, the integration of Thermal Storage Wall (TSW) in the building envelope can be a practical solution to the heating problem. These walls are located in the south face of buildings and are built from materials with a high heat absorption property. Thermal storage wall is more efficient in climates with a large difference in temperature throughout day and night, which is also common in Cyprus.

Recent study [1] have shown that improvement in the performance of TSW performance can be achieved by creating changes in the material used and TSW dimensions. Fan Wang [1] investigated the solar wall systems used in domestic heating. In his study he discovered that the wall absorbed heat during daylight and delivered the heat to a living space during night time. In his study, the temperature distributions inside the wall were measured daily.

The previous designs have not adequately used additional equipment to enhance the performance of the TSWs.

The rooms with TSW do not have heating difficulties. The problem is to solve heating difficulties in rooms which are located in the north side of buildings. Installing an array of pipes on the TSW surface and transferring heat to water which passes through pipes and pumped to the rooms in the north side can solve this problem. As a result, with a hybrid TSW-water heating system the heating of rooms which are located both in south and north side of the building may be possible.

The aim of the present work is to investigate the performance of the existing TSW, with water pipes attached to it. The thesis is organized as follows:

In chapter 2, literature on TWSs is reviewed. The laboratory room is described in chapter 3. In chapter 4, the mathematical parameters and the methodology is described. In chapter 5, the setup and the procedure of the experiment are described.

In chapter 6, the results of the experiment are presented and discussed. In chapter 7 the conclusion on experimental outcomes is made and the related future work is suggested.

Chapter 2

LITERATURE REVIEW

Trombe wall systems were utilized for the first time by Edward Morse in 1885. Next step in its development was an experimental house in Odello, France by Felix Trombe and Jacques Michel [2]. Passive solar system and thermal storage wall become an important issue and it assigns several theoretical and experimental investigations subject to itself.

The literature on thermal storage wall and passive solar-wall systems will be discussed in this chapter.

A simulated and experimental performance of a heat pipe assisted solar wall has been done by Albanese and Robinson in University of Louisville. Performance was estimated for a passive solar space heating system which uses heat pipes to transmit heat through the wall to a storage tank located inside the home was estimated by means of an experimental study. A computer model was also developed. The simulation results were compared with the experimental results. In the experimental work by insulating heat pipes the efficiency was improved to approximately 85%. The simulation results showed that the absorber thickness, material selection and the number of covers had little effect on system efficiency. Whereas, cover thickness, thermal storage capacity, extinction coefficient and absorber surface properties were parameters which had profitable effects on system efficiency[3].

The optimum design of Trombe wall system in Mediterranean region has been studied by Jaber and Ajib. Thermal impact of TSW for residential buildings in this region has been studied. By using Life Cycle Cost analysis, the optimum size of Trombe wall system is determined. In addition, the performance of Trombe wall is analyzed with TRNSYS program to estimate the hourly heat energy supplied. It is found that Trombe wall system does not decrease the maximum heating load but it reduces the annual energy consumption of a building.[4].

Energy analysis of buildings employing thermal mass in Cyprus has been studied by Kalogirou. TRNSYS program is used to modeling and finding the effects of thermal mass on the heating load of a typical home with an insulated roof. The simulation result demonstrates that the heating load requirement decreases approximately about 47%. In addition, different construction parameters such as the best overhang size should be around 1.2 m and also the most advantageous value of wall thickness estimates is approximatly 25 cm. According to this paper the effect of roof insulation is a necessary action for providing better condition inside the home. In addition, utilization of ventilation in summer season is estimated to decrease the building cooling load [5].

An experimental work with mathematical study on novel photovoltaic- Trombe wall (PV-TW) has been done by Ji Ji et al. In this study, two identical test rooms, one with PV and the other without are prepared for comparing the results. The one without the PV is called the reference room. The effect of the PV-TW on the room thermal condition was considered. The results showed that the temperature inside the test room is increased by approximately 5-7 ˚C during winter weather in comparison with the reference room. In addition, with a surface area of 0.72 m^2 for PV cell the daily electrical output is estimated 0.3 kWh [6].

Another experimental evaluation has been done on the energy performance of concrete wall integrated with mini solar collectors by L.A. The energy performance of Trombe wall is estimated throughout the whole year. The panel includes two different type of concrete that the normal- weight concrete layer is used in interior surface and the lightweight concrete layer with the density of more than 1000 kg/m^3 is used in exterior wall surface. As shown in Fig 2.1, a solar thermal collector surronding10% of wall surface is embedded in the outer wall surface. According to this study the efficiency of the system was approximately improved by 15% [7].

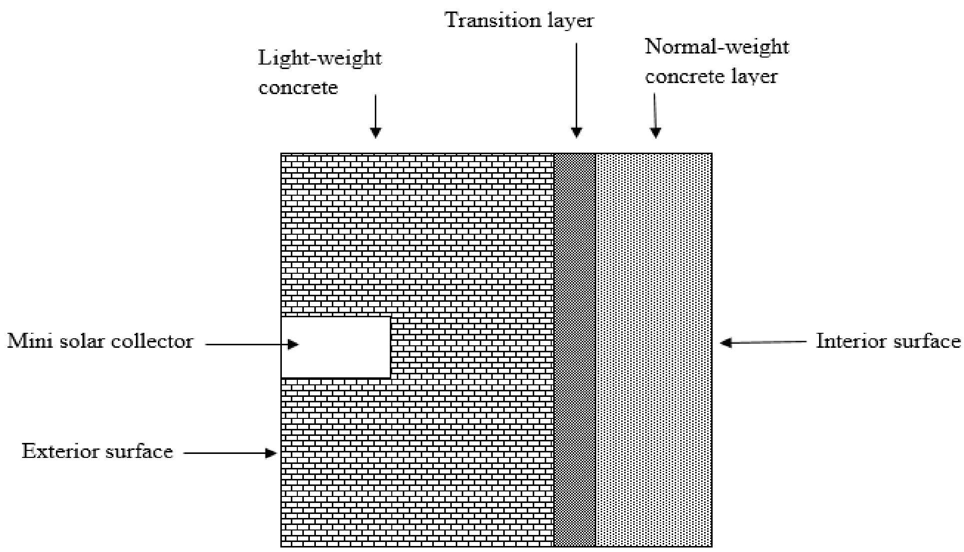

Figure 2.1. Horizontal section through wall panel previously displayed in Ref. [7]

Kara et al. has studied a phase change material on a Trombe wall to estimate the efficiency of double novel triple glass and Trombe wall. Trombe wall is built on the south face of the test room which is divided in two parts. One part is made of GR35 plaster boards and the other on is made of GR41 plaster boards that are shown in Fig

2.2. The results illustrated that the daily overall efficiency of phase change material wall including GR35 was higher than the GR41. In addition, the total solar radiation absorbed by phase change material wall was approximately 36%, but the solar transmittance of the novel triple glass reached 0.55 [8].

Figure 2.2. The test room used in experimental project of Ref. [8]

Fang Wang et al. has studied the feasibility of TSW in domestic utilization. In this project there is a laboratory model which integrated with solar water system to investigate the dynamic efficiency of the system. The temperature distribution inside the wall during a day was measured. This paper illustrates the modeled results of the TSW and optimization system in a typical flat in the Scottish weather. The investigation demonstrates that this system can be used both in domestic hot water and heating the house space especially in buildings with heavy thermal mass. Moreover, economic analysis illustrated approximately 16 years payback period [1].

An experimental and theoretical study of Trombe wall heat transfer had been done by Smolec et al. in Indian institute of science. The aim of this paper is to forecast the heat transfer in TSW based on the uniform temperature distribution assumption inside the wall in one direction for calculation of wall convection heat transfer. In this paper with different assumption for the heat transfer coefficient to achieve a settlement between theoretical and experimental data, results illustrate that the convection heat transfer in vented Trombe wall depends on the distance from the bottom vents [9].

The performance of a solar wall with heat pipes has been studied by Robinson et al. in Louisville University during a spring season. The efficiency that calculated in this study was 83.7% for maximum daily thermal performance and 61.4% for the average daily peak thermal performance. The maximum gain was 163 W/m^2. The experiments conducted on clear and sunny days with profitable solar radiation is showed the performance of Trombe wall is increased in these days. The average of 4 days hourly heat delivered to the classroom from the tank was positive, and the lowest value was 16.6 W/m^2. As a result, with good insolating TSW temperature was restored quickly to suitable levels [10].

The energy performance of TSW adapted with ISO has been studied by Ana Briga-Sa et al. in Beira Interior University. The aim of this study is to investigate the most effective factors on thermal storage wall performance suitable to the Portuguese weather. It is considered that the global heat gains are transferred by conduction, radiation and convection. In addition, installing a ventilation system in TSW has a major role in the thermal storage wall performance. According to this study by integrating a Trombe wall in building envelope the energy heating demands decreases around 16.36% in Portuguese residential buildings [11].

Yilmaz et al. has studied the performance of Trombe wall in residential buildings as an alternative energy conscious in Istanbul. Turkey suffers from the lack of fossil fuels the same as Cyprus. On the other hand, it has a profitable solar energy potential. According to the information 36% energy consumption belongs to heating the buildings. In this study, Trombe wall applied to a south face of an existing building. The hourly temperature distribution inside the wall was measured. The results illustrate that creating changes in wall materials has not considered effects on thermal storage wall performance. In addition, a new method for the renewal of the building facades with TSW is introduced in this project and finally the collecting data for two different approaches is compared together. In Figure 2.3 the heat gains and losses of the TSW and renovates wall without glass cover is shown [12].

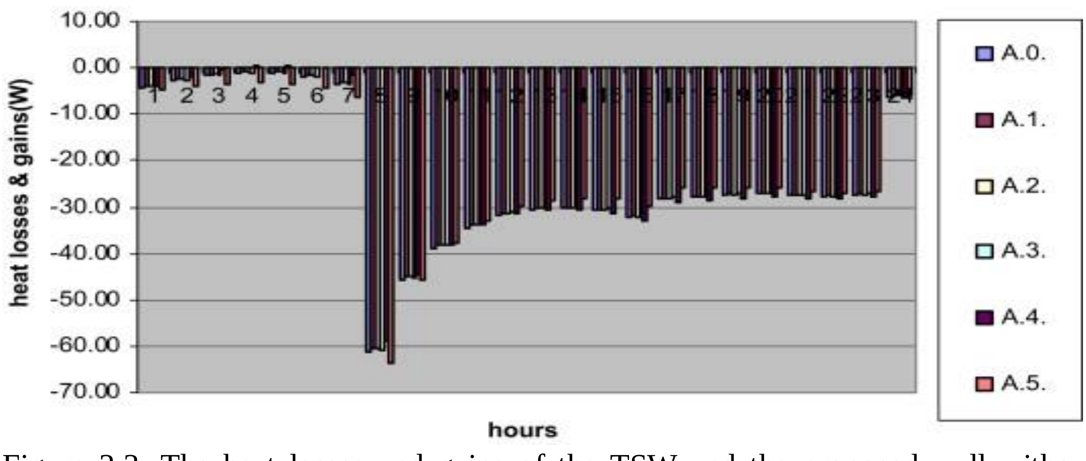

Figure 2.3. The heat losses and gains of the TSW and the proposed wall without glass cover previously displayed in Ref. [12]

A basic and economic investigation about TSW has been done by Omidreza Saadatian et al. In this new investigation the different types of Trombe wall which combined with new architectural design and the advantages and disadvantages of the TSW are discussed. In addition, the effect of different factors includes insulation; thickness of TSW on the annual heat gain is investigated in this study [13].

As the environment problem became an important issue, the numerous studies have been done to improve the performance of the sustainable buildings and technology like TSW. In order to encourage homemaker to integrate TSW in building construction, obvious economical study which shows the feasibility of the new technology is a necessary action.

Parallel to this issue Javad Eshraghi et al. has been study a feasibility of integration a solar energy for a typical building in Tehran. The aim of this study is to investigate the economic analysis of building a zero energy house which is includes TSW, thermal mass, roller shading, and solar absorption pump to supply heating and cooling requirement. In this project the rate of released CO_2 to the environment is estimated per home. The result illustrates that just with actual energy price and considering at least interest rate this project is feasible [14].

Normally to overcome the long warm up time in the morning which is caused by a night without sunlight, four vents are placed to increase the performance of the TSW. The air is heated by convection and rises and passes into the heated space through openings in the vents at the top. The displaced air is replaced by air of lower temperature in the room through the bottom vents of the masonry wall. A quicker warm up time in the morning is achieved by convection which is continued until conducted heat throughout the wall surface is started. At night time the outer wall surface temperature and gap space temperature is decreased even less than room temperature. The coolest air agglomerate in gap space and caused “reverse thermo circulation” between the gap and room space. As a result, this event leads to lose all the heat gain which is conducted through the wall to the room space by top vents (Figure 2.4). For preventing of the reverse thermo circulation at night time, shutting the vents off during this time is a compulsory action. Considering, in this project during the experiment all the vents have been closed [2].

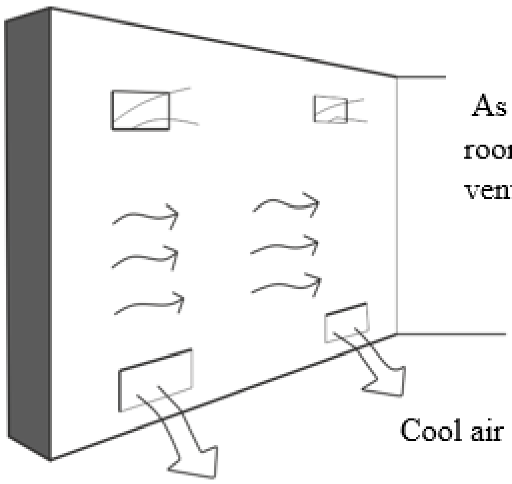

Figure 2.4. Reverse thermocirculation in vented Trombe wall at night time [2]

In this research, thermal behavior of the TSW embedded in solar energy laboratory is investigated. The motivation of this study is to observe the performance of hybrid TSW-water heating system during one of the coldest month in Cyprus.

Chapter 3

SOLAR ENERGY RESEARCH INSPECTION AND TRAINING (SolERIT) LABORATORY

A 10 m^2 building was built just outside the heat transfer laboratory of the Department of Mechanical Engineering for the purpose of conducting experiments in solar energy and training professionals. There is also an opportunity to perform tests for solar collectors for certification purposes. The roof of the building is inclined at two different angles to allow maximum performance for photovoltaic (PV) and solar thermal panels as can be seen in Figures 3.1 and 3.2.

Figure 3.1. Front view (South façade) of the SolERIT Laboratory

The cross-section of the SolERIT laboratory – as it was designed originally – is shown in Figure 3.2. As it can be seen from this drawing the building incorporates a TSW facing to south.

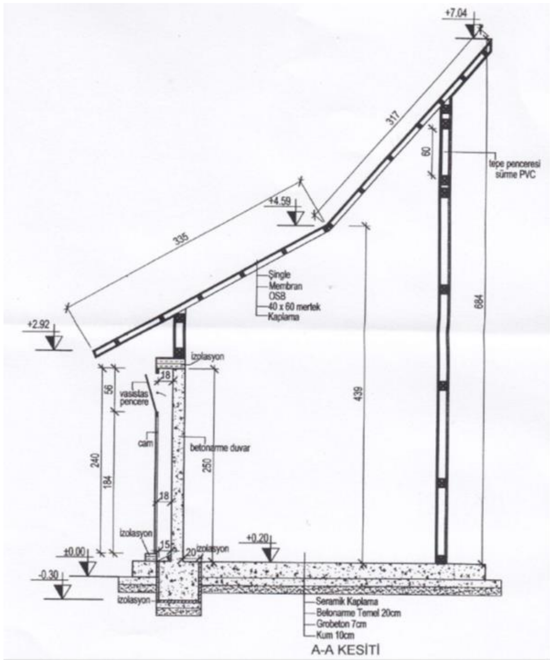

Figure 3.2. Cross-sectional view of the SolERIT laboratory

The SolERIT Laboratory is designed to have 10 m^2 total floor area of as illustrated in Figure 3.3.

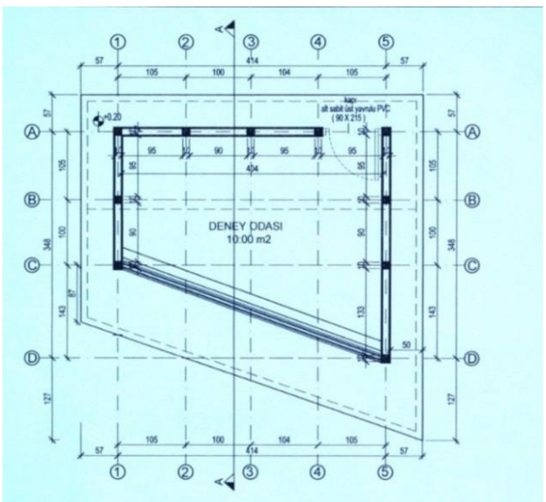

Figure 3.3. Plan view of the SolERIT Laboratory

Steel framing is used to construct the SolERIT Laboratory. Sidings made of cement were used from the outside while PVC panels were preferred in the indoors to cover the frames. Furthermore, it has a window of 0.638 m^2 floor area and entrance door facing to North. The laboratory also incorporates a TSW made out of reinforced concrete and is painted in black on the outer surface to absorb solar insolation. The TSW is designed to have 8.073 m^2 of solar exposure area and 16 cm thickness. Moreover, Table 1 illustrates the TSW characteristics used in this project. TSW are "sluggish" and need time to conduct heat through itself to inside in the morning. Normally to overcome the long warm up time in the morning which is caused by night without sunlight, four vents are placed to increase the performance of the TSW [2]. The vents are illustrated in Figure 3.4.

Table 1. Characteristics of the TSW of the SolERIT Laboratory

TSW characteristics	
Height	2.46 m
Width	4.16 m
Thickness	0.16 m
Specific Capacity The product of the Trombe wall density and wall specific heat	0.653 kj/kg.K
Number of glazing in front of Trombe wall	1
Space between wall and glazing (gap size)	0.15 m

Glazing window is another important subsection of TSW, which is installed against concrete wall with an air space to preserve the external wall surface from the environment and it has 9.954 m^2 surface areas. An aluminum frame held all around the glass in order to keep the glass part. Figure 3.4 show the glazing and its dimensions.

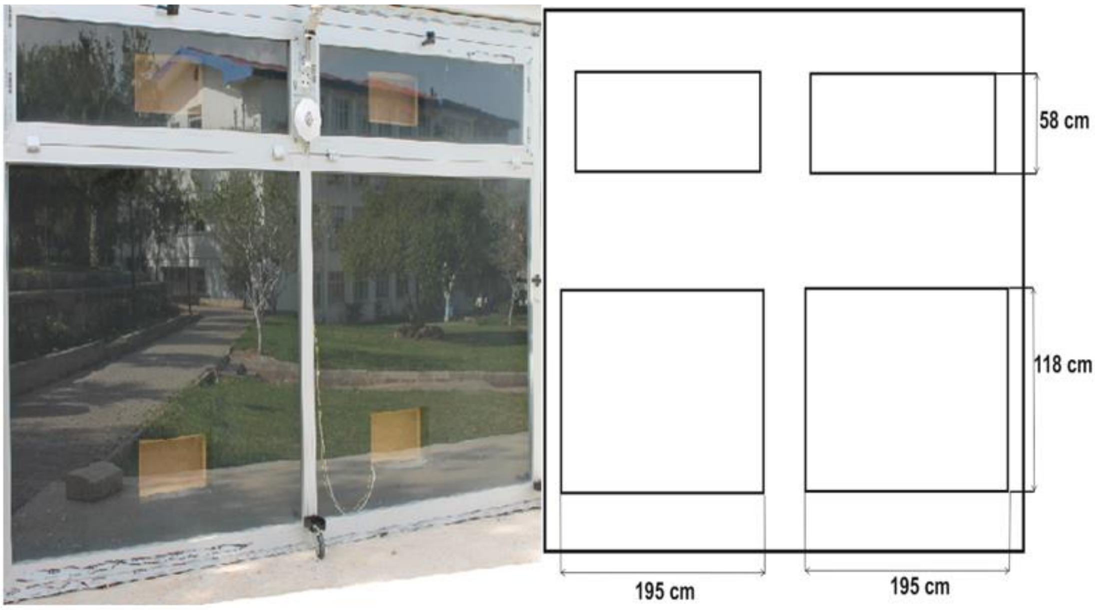

Figure 3.4. Glazing, vents and aluminum frame of TSW

The efficiency of Trombe wall could be enhanced if the suitable insulation is utilized in the system. As a matter of fact, existence of insulation is an essential parameter in passive solar buildings. Despite of this knowledge, the energy laboratory was built without thermal insulation. The foundation of the TSW was thermally insulated with 3cm-thick extruded polystyrene foam.

Chapter 4

EXPERIMENTAL INVESTIGATION

The SolERIT Laboratory described in the chapter 3 is used for this experimental study. In this chapter the equipment installation in the SolERIT Laboratory for the purpose of performing this study is explained. Moreover, the experimental procedure adopted is described.

4.1 Experimental Set up

An array of water pipes is fastened on the TSW with the intention of capturing solar energy to heat the circulating water through them for using in low-temperature applications. It is desired to measure the inlet and outlet water temperatures of this array of pipes, which is also referred to as the collector. Therefore K-type thermocouples are inserted in the inlet and outlet of the pipes. A flowmeter was used to measure the flow rate. Thermocouples were also inserted into the wall at different depths (4 cm apart from each other) to monitor the temperature distribution inside the cross-section of the wall. All the data collected from the thermocouples together with the solar radiation data obtained by a pyranometer is collected in a computer, through a data logger.

A schematic diagram of the experimental set up used for carrying out the experiments can be seen in Figure 4.1. The details are explained in the following sections.

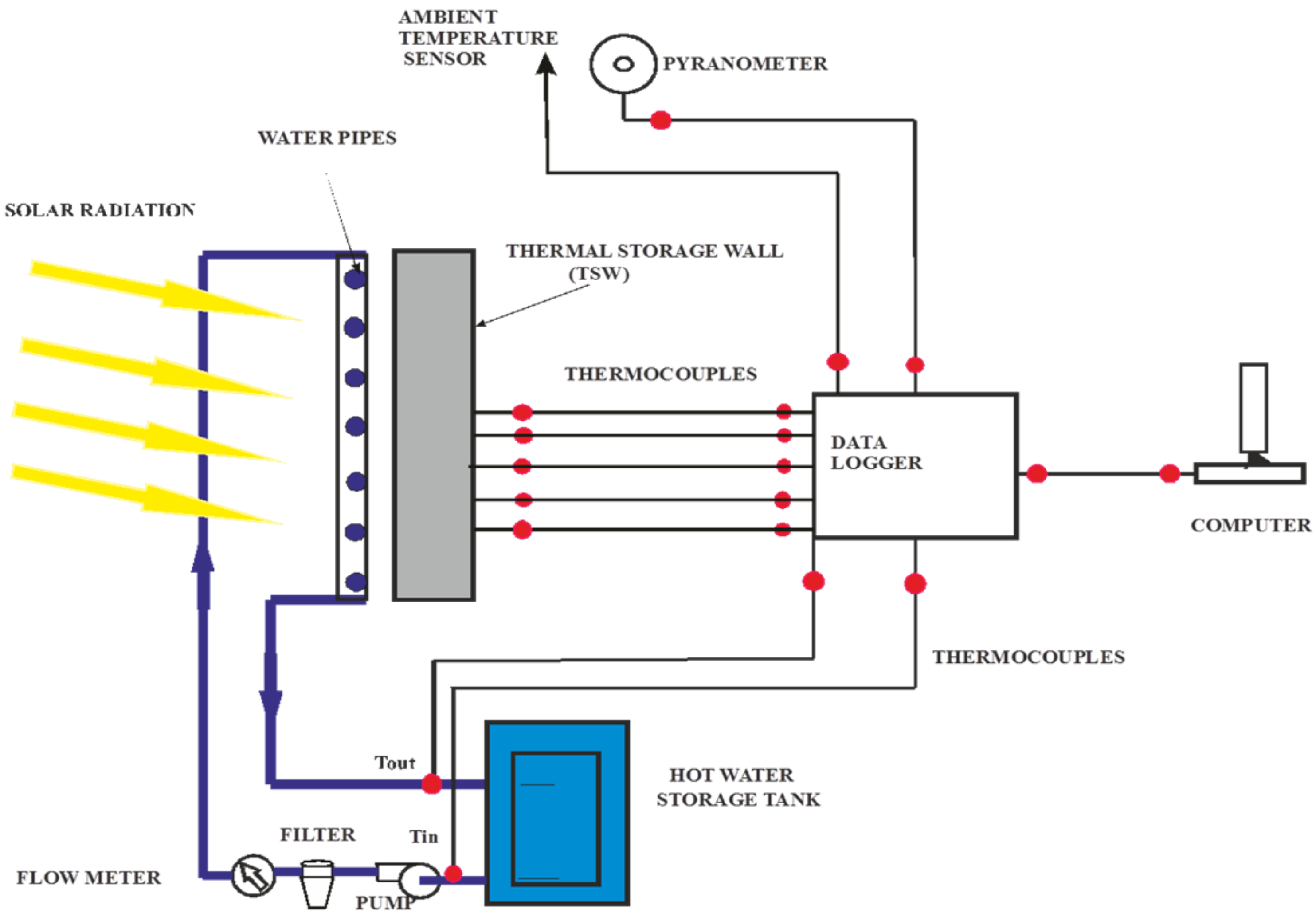

Figure 4.1. Schematic diagram of experimental setup

4.1.1 Water copper pipes system

The pipes used in the air gap (between TWS and the glass) are copper. They are installed on the surface of the TSW. The pipes are painted in black for maximum absorption of solar energy. The technical drawing of the water copper pipes is provided in Figure 4.2.

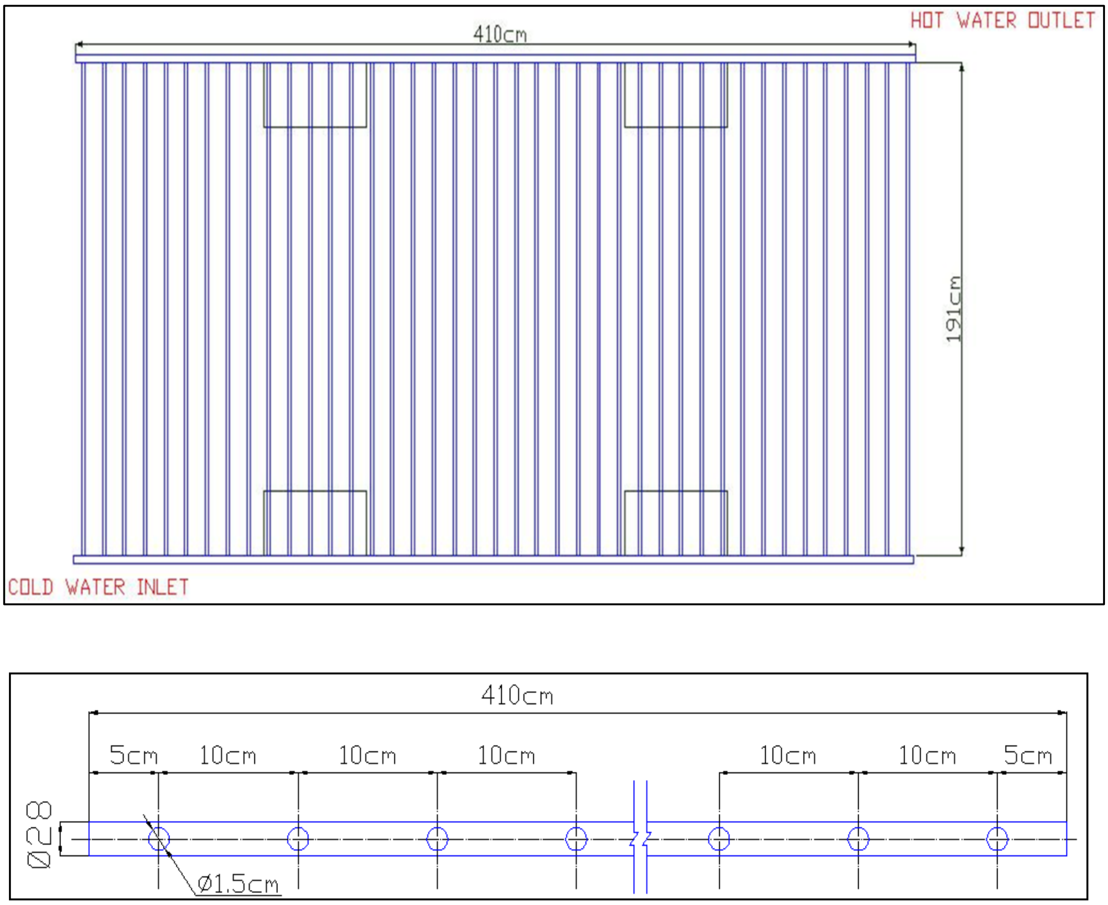

Figure 4.2. Water pipes

The inlet water which is at room temperature is pumped from the bottom of a tank of 1 m^3 volume, and the outlet water is returned to the top of the tank. In order to protect the high precision flow meter from getting damaged a 20 micron filter is installed before it. The flow rate of water can be changing by placing pump in three different steps. The water flow rate can be varied further by a valve which is installed after the flow meter. The Connection of the pump, 20 micron filter and the flow meter is shown in Figure 4.3.

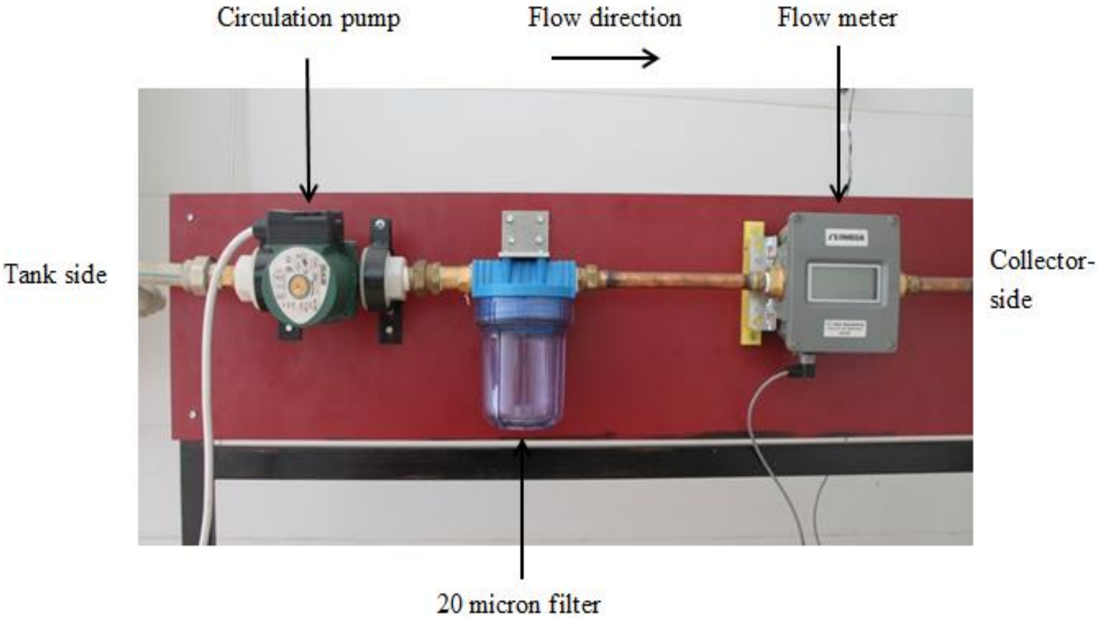

Figure 4.3. The connection of circulation pump, 20 micron filter and the flow meter

The main reason of installing pipes on the surface of the TSW is to investigate the rate of heat collected by water collector on the system efficiency and also the capability of warm water utilization for domestic purpose. In order to measure the water temperature two thermocouples are installed in the inlet and outlet of the pipes. These two thermocouples connected to the data logger or data acquisition to record data in the laboratory computer.

4.1.2 Thermocouple connections on TWS

Thermocouples are temperature measurement and self-powered devices. They have various class forms of temperature sensors. In this project "K" type of thermocouple is used. The K type of thermocouple which is made of two different materials (chromel –alumel) is the most popularly used general intention thermocouple. In addition, the room temperature is measured by the same type thermocouple.

In order to find the temperature distribution inside the TSW, the TSW with thickness of 0.16 m is divided into four equal horizontal sensor layers. The thermocouples placement initiated from the outer wall surface and then passes through the thickness of the wall into the inner wall surface. The thermocouple placements inside the TSW are illustrated in Figure 4.4.

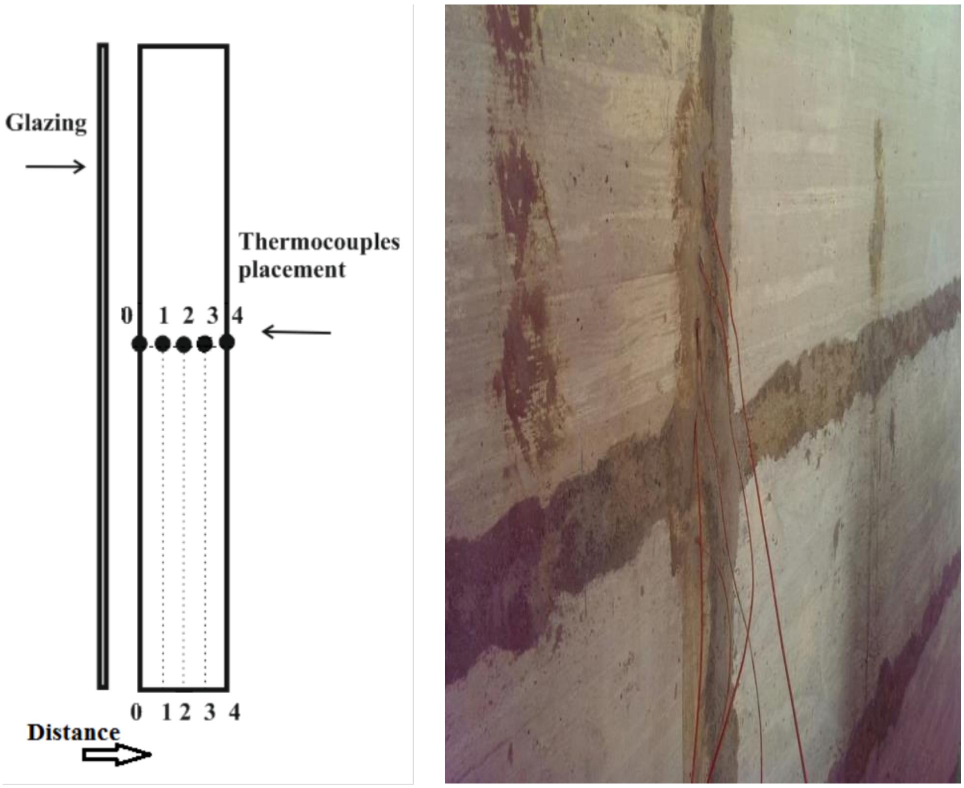

Figure 4.4. The cross section area of TSW and thermocouples placement.

In order to record the data all the thermocouples inside and outside the TSW are connected to the data logger.

4.1.3 Data acquisition

Data acquisition (DAQ) is a device that polling signals and evaluates actual world physical situations and changing the resulting examples into digital numeric standards that can be used by a computer. The type of data acquisition which utilize in this project is OMB-DAQ-3000 Series which is shown in Figure 4.5. All the thermocouple applied in Trombe wall and water pipes system have been connected to the data acquisition. DAQ directly connected to the computer in order to show the collected data by thermocouples. In total, there are eight thermocouples which connected to the data acquisition. It is noticeable that, calibrating of DAQ before operating is a necessary action.

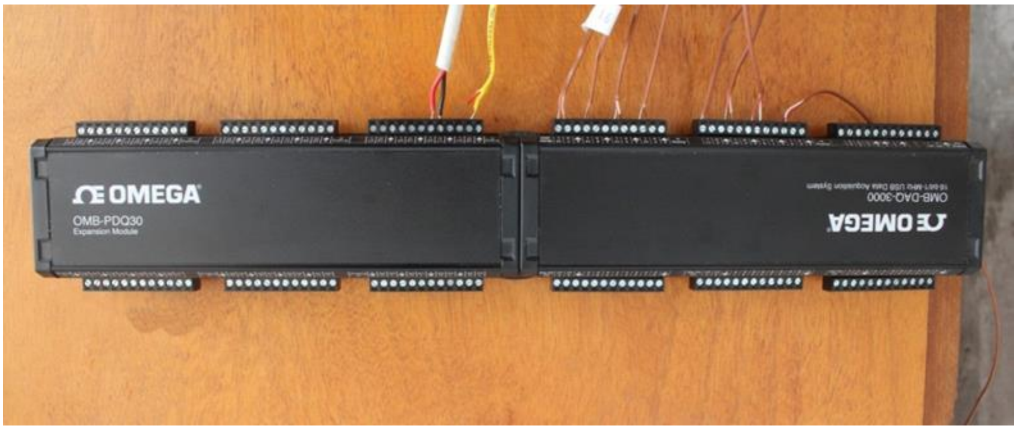

Figure 4.5. Data acquisition system

4.1.4 Pyranometer location

Pyranometers are sensors to measure the solar radiation on planar surfaces. They standardized corresponding to the ISO 9060 standard and also calibrated according to World Radiometric Reference (WRR).

Pyranometer has a thermopile sensor that covered with black color and absorbs the solar radiation. After this step, the solar radiation absorbed by the black coating converted to heat. In addition, it can be fixed individually or as a section of a meteorological station in order to measure the temperature, wind speed and relative humidity. In this project, the pyranometer has an accuracy of ± 0.5 for the range between 0 and 2800 W/m^2 which is shown in Figure 4.6.

In order to decrease the errors in measuring for receiving solar radiation from unnecessary direction, the pyranometer should locate horizontally parallel on the wall surface.

4.1.5 Ambient temperature sensor

Ambient temperature sensor is a device to measure ambient humidity and temperature. In this project just the outside temperature is measured. The type of this sensor used in this project is radiation protection shield. Figure 4.6 shows the model of ambient temperature sensor used in this project.

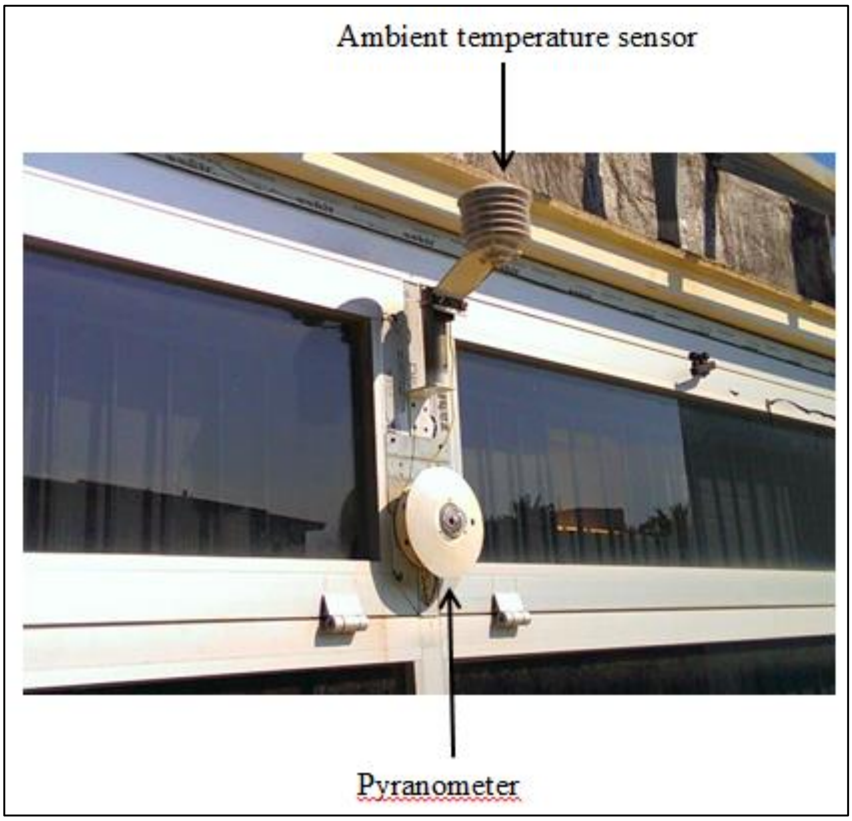

Figure 4.6. Pyranometer and ambient temperature sensor with radiation protection shield.

4.1.6 Flow Transmitter

The FLR Flow Transmitter is capable of calculating and displaying both flow rate and total accumulated flow/ the flow rate and total flow can be displayed in any of the user selectable measurement units. The accuracy of the equipment is $\pm 2\%$ of full scale. The flow transmitter brand is Omega and from the FLR5000-9000 series.

4.2 Experimental Procedure

Recording data is conducted on selected days in March 2015 which is one of the heating months in Cyprus.

The DAQ system which is connected to the laboratory computer recorded data belongs to temperatures and solar radiation one time in each twenty minutes. The pump is operated at approximately 8:00 for each day. It is important to run the water through the pipes in order to achieve a steady state flow before taking the readings. Therefore, to prevent from recording incorrect data, the data collection is started at 8:20. Depending on the solar radiation the water flow rate is adjusted to obtain favorable outlet temperatures. For example in clear days the pump is adjusted to the third step to achieve the maximum flow rate and in cloudy and rainy days the water flow rate is decreased by adjusting the pump to the first and second step. The water flow rate changed slightly due to temperature and pressure changes during the day. Therefore the flow rate is recorded every two hours and average is evaluated to make use of in the calculation.

Water absorbs solar radiation during its circulation through copper pipes which is installed on the exterior surface of the TSW before it is returned to the top part of the tank. Moreover, in the tank the warm water stay on the top level for a long time without mixing with the cold water. Therefore, there is a separation line between the warm and cold water in the tank which is also known as a “thermocline” [15].

The pump operation is stopped at 14:40 when the solar radiation disappeared from the outer TSW surface. Therefore at this time water circulation is stopped through the pipes and it is considered that the rate of heat which collected by water collector is zero after 14:40.

Although, after the hour of 14:40 the water circulation is stopped, but measuring the ambient and room temperature and temperature distribution inside the wall are continued and recorded by DAQ system. Therefore, the experiment is continued for 24 hours.

Chapter 5

MATHEMATICAL PARAMETERS

5.1 Heat gain by water

It is sought to investigate the useful energy absorbed by the circulated water and the heat transferred by the wall. For this reason it is necessary to introduce the mathematical equations used in the analysis.

Water pipes are arranged in such a way that water is circulated from the storage tank and passed through them as they face south to collect the solar energy. Heat transfer by water pipes to the system is evaluated by the following equation [15]:

$$\dot{Q} = \dot{m} C_p \left(T_{o,w} - T_{i,w} \right) \quad (1)$$

where $\dot{m}$ is the mass flow rate of the circulating water and C_p is its specific heat capacity.

In addition, due to the range of low temperature difference in the project, the value of C_p has been considered constant. The $T_{o,W}$ and $T_{i.w}$ are the water temperatures at the outlet and the inlet of the collector respectively.

5.2 Heat delivered by TSW

Solar radiation is absorbed through outer wall surface and transmitted by conduction through the wall thickness, and gradually reaching the inner wall surface (Figure 5.1). Heat transmission from inner wall surface to the room space is by radiation and convection.

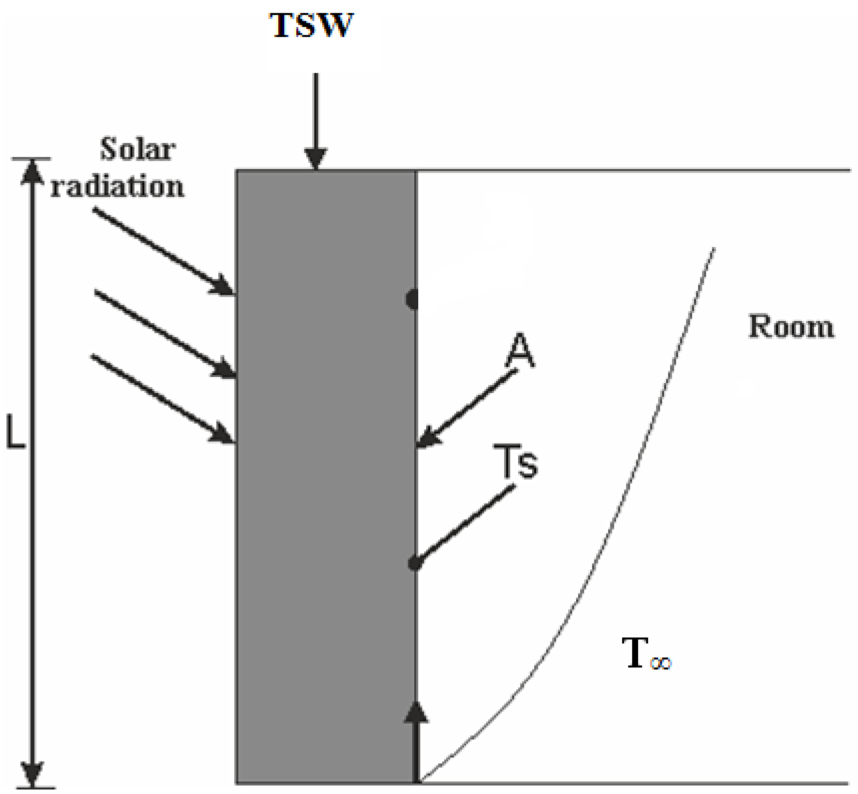

Figure 5.1. Natural convection flow through the TSW

Due to absence of forced air movement, the heat convection losses from the wall surface to the room space can be considered as natural convection. Natural convection is only as executable in the heating of low temperature surfaces which is placed in the warmer space and also for the loosing heat from hot surfaces in a cooler space. Natural convection heat transfer from a surface appertains to the surface orientation. Furthermore, it depends on the temperature difference between wall surface and room air temperature. In order to increase the accuracy of estimating convective heat transfer (Nu) was evaluated [16].

Rather complex but reasonably accurate experimental correlation for the mean Nu for natural convection on the surfaces is defined as follows [16]:

$$\text{Nu}=\left\{0.825+\frac{0.387 Ra_L^{1/6}}{\left[1+\left(0.492/\text{Pr}\right)^{9/16}\right]^{8/27}}\right\}^2 \quad (2)$$

where Ra_L is the Rayleigh number, which is given as:

$$Ra_L=Gr_L Pr \quad (3)$$

where Gr and Pr are the Grashof and Prandtl numbers.

$$Gr_L=\frac{g\beta\left(T_s-T_\infty\right)}{\upsilon^2}L^3 \quad (4)$$

$$\text{Pr}=\frac{\nu}{\alpha} \quad (5)$$

where g is the gravity of Earth, and β is $1/T_f$ and T_f is equal to $T_s+T_f/2$. In addition, ν is the dynamic viscosity and α is molecular diffusivity of heat.

Finally the value of mean heat transfer coefficient on the wall surface, h, will be determined from the following standard equation of Nusselt number:

$$\text{Nu}=\frac{hL}{k} \quad (6)$$

where the k is thermal conductivity in W/m . K.

The rate of heat which is transferred by natural convection from wall surface at uniform temperature to the room space is expressed by Newton cooling's law as:

$$\dot{Q} = hA_s(T_S - T_\infty) \tag{7}$$

where A_s is the heat transfer area and T_s is the inner wall surface temperature, T_∞ is the room temperature, and h is the heat transfer coefficient.

The value of h depends on the film temperature, which is illustrated as T_f and is equal to (T_∞ +$T_{s)}$ /2. It is known that h is a function of Nu and the value of Nu depends on the Ra_L. In addition, according to equation (3) the Reyleigh number is a function of Prandtl number and Gr which are depends on the film temperature. Since during one day 73 recording are taken, calculating h becomes a laborious work. h was evaluated for each recording by writing a program in MATLAB software. The details of the written program are available in Appendix.

For example, for surface and room temperature of 32.2 and 28.1 °C respectively, h is evaluated to be approximately 2.7 $W/m^2.°C$.

Using Eq. (7) $\dot{Q}$ was evaluated to be 111.244 W.

The TSW surface area is around 10.23 m^2; though due to shadow which caused by aluminum frame the neat area of TSW is considered as 8.073 m^2.

The net heat transferred from wall surface to the room space by radiation has been expressed by the Stefan-Boltzmann law as:

$$\dot{Q} = \varepsilon\sigma A_s\left(T^4{}_{i,Tw} - T_{i,r}{}^4\right) \tag{8}$$

where ε illustrates the emissivity of the wall surface and the assumed value of emissivity in this project is equal to 0.9 , σ is the Stefan-Boltzmann constant and is equal to 5.670×10^{-8} W/m^2. A_S denotes the wall surface area (m^2). $T_{i,Tw}$ is the inner wall temperature and $T_{i,r}$ is the room temperature in K.

To make it more clear the following example is given as follows for calculating the radiation heat transfer from wall surface to the room.

On the 10th of March 2015 at 15:40, the TSW inner surface and room temperatures are equal to 38.20 $°C$ and 30.5 $°C$ respectively. The heat transferred from wall surface to the room by radiation has been calculated as below:

$T_{i,Tw}$ =38.20 ˚C

$T_{i,r}$ =30.5 ˚C

The temperature should convert to the kelvin. Therefore,

$T_{i,Tw}$ =38.20 ˚C+273 K=311.2 K

Using Eq. (8) $\dot{Q}$ was evaluated to be 454.3 W.

5.3 Efficiency

Daily heat transfer efficiency of the TSW is defined as the heat delivered to the room in one day divided by the solar heat gained. The heat stored in the TSW which is not utilized in that day is not taken into account. Mathematically it can be expressed as follows:

$$\eta_{TSW} = \frac{Q_{radiation} + Q_{convection}}{SA_s} \qquad (9)$$

where S is the total solar intensity (W/m^2) falling on to the outer surface of TSW.

The efficiency of the solar collector for heating water is calculated as follows:

$$\eta_W = \frac{Q_w}{SA_s} \tag{10}$$

The total efficiency of the system is evaluated from:

$$\eta_{tot} = \frac{Q_{radiation} + Q_{convection} + Q_{water}}{SA_s} = \frac{Q_{Total}}{SA_s} \tag{11}$$

The numerator indicates the total heat delivered into the room by convection and radiation, and the heat collected by the water pipes system, and the denominator denotes the total energy read by the pyranometer.

5.4 Error analysis

In this section errors related to the experimental equipment is presented. The uncertainties for the water collector and total efficiency due to water mass flow rate, temperature and solar intensity are briefly described next.

K-type thermocouples with $\pm 0.4\,\%$ accuracy were used in this project. Furthermore, the accuracy of pyranometer and mass transmitter used in this study are $\pm 0.5\,\%$ and $\pm 2.5\%$, respectively.

Assume a set of measurements is made and the uncertainties for each measurement are expressed as $\omega_1, \omega_2, \ldots, \omega_n$. If the result R is a given function of the independent variables $x_1, x_2, x_3, \ldots, x_n$. then the uncertainty in the result is defined as follow equation [17]:

$$\omega_R = \left[\left(\frac{\partial R}{\partial x_1} \omega_1 \right)^2 + \left(\frac{\partial R}{\partial x_2} \omega_2 \right)^2 + \ldots + \left(\frac{\partial R}{\partial x_n} \omega_n \right)^2 \right]^{1/2} \tag{12}$$

Then, the uncertainty of water collector efficiency and total efficiency is calculated as follow equation, respectively [18]:

$$\frac{\varepsilon_{\eta}}{\eta}=\left[\left(\frac{\varepsilon_{m}}{m}\right)^{2}+\left(\frac{\varepsilon_{\Delta T}}{\Delta T}\right)^{2}+\left(\frac{\varepsilon_{I}}{I}\right)^{2}\right]^{1/2} \tag{13}$$

$$\frac{\varepsilon_{\eta}}{\eta}=\left[\left(\frac{\varepsilon_{\Delta T_{Convection}}}{\Delta T_{Convection}}\right)^{2}+\left(\frac{\varepsilon_{\Delta T_{Radiation}}}{\Delta T_{Radiation}}\right)^{2}+\left(\frac{\varepsilon_{I}}{I}\right)^{2}\right]^{1/2} \tag{14}$$

Chapter 6

RESULTS AND DISCUSSION

Experiments were conducted on selected days with different weather conditions in March, which is one of the heating months in Cyprus. The aim is to investigate the performance of TSW and the hybrid TSW-water heating system in alternative weathers, separately. Additionally, the effect of solar radiation on the temperature distribution in the wall cross-section and the room temperature are analyzed.

The solar radiation and temperature measurements were recorded every twenty minutes starting at 8:20 on each day. As it can be seen from Figure 6.1 on 10th March, 2015 there was a clear weather with a full profile of solar radiation. However, on the 11th March the weather was rainy and the T_a falls from 15 to 10 °C. The measured temperatures of all thermocouples are also plotted against time in a day in Figure 6.1.

It is observed from Figure 6.1 that the weather for the two consecutive days (10th and 11th March 2015) can be described as “sunny” for the first and “rainy” for the second day. On 10th March, although T_a was measured to be 19 °C at 8:20, it gradually reached a maximum value of 26.5 °C at 11:20. On the other hand, T_r was recorded to be 20.9 °C at 8:40 rising to a maximum value of 31.30 °C at 11:00 and then retreating exponentially during the night to 22.7 °C at7:00 next morning (i.e. on 11th March).

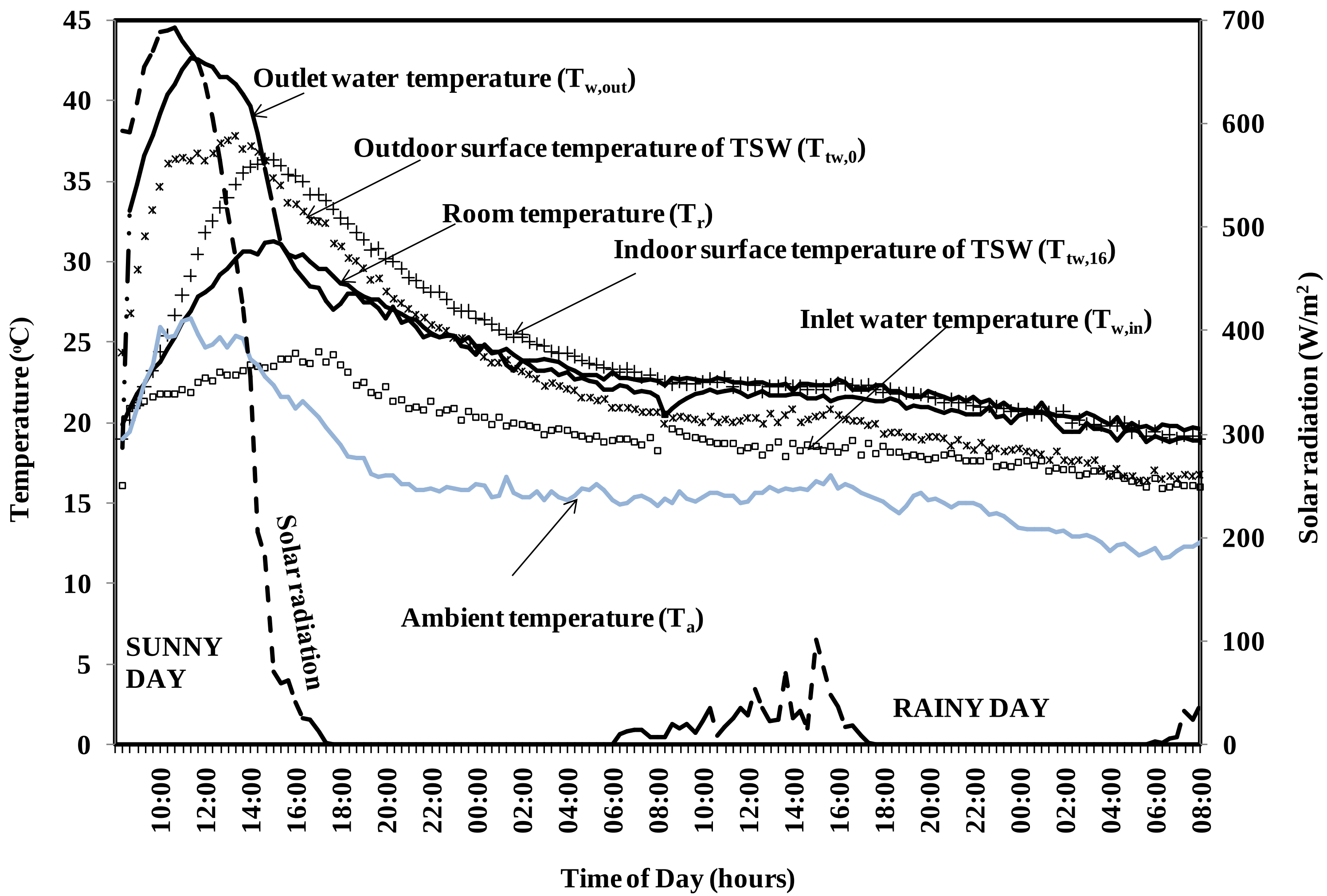

Figure 6.1. Solar radiation and temperatures measured as a function of time recorded on the 10th and 11thMarch2015.

On the next day (11th March) there was hardly any radiation (S_{max}=101.6 W/m^2 at 15:00) and T_a varied between 16.7 °C and 13.5 °C until mid-night. After mid-night it fell slightly to 11.6 °C at 6:20 in the morning of 12 March. T_r on the contrary, maintained a level of 7-9 °C higher than T_a. This is due to the energy stored in the TSW. TSW continued to emit heat into the room throughout the rainy day of 11th - 12th March.

It is also noticed that the peak values of solar intensity and T_a take place at almost at the same time. However, the peak value of T_r is reached 4 hours and 20 minutes later on 10th March 2015. This shows that TSW heating systems operate in a delayed action process with stored energy for later.

The time at which the recording is started (i.e. 8:20) until the room temperature peaks is assumed to define the solar heating period (Figure 6.2). During this period the outer surface temperature of the wall ($T_{tw,0}$)increases and becomes higher than the inner surface temperature ($T_{tw,16}$). This period continued until 14:40. At this time, the shadow from the trees appears on the wall surface and the cooling time is commenced. The outer surface temperature of the wall becomes less than the inner surface temperature, even lower than the wall interior temperatures. Figure 6.2 displays the inner and outer surface temperatures of TSW on 10thMarch.

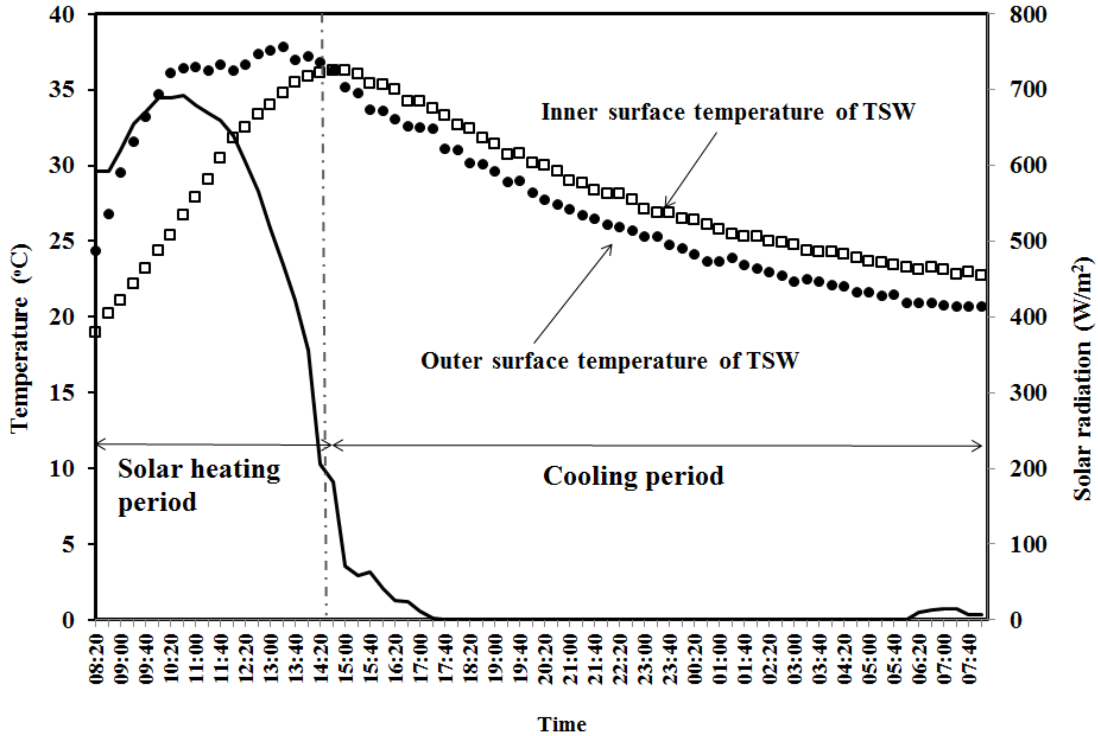

Figure 6.2. The inner and outer surface temperature of the TSW.

According to Figure 6.2 the cooling process of the outside surface of the TSW $(T_{tw,0})$ starts precisely after sunshine moves away from the TSW surface. Subsequently, we found that the gap between the wall and the glass is not air tight and the cold wind enters from the right edge of aluminum frame. In addition, because of the typical glazing used on the outer wall surface, heat losses are maximized.

Since, the weather was clear and sunny on 10thMarch; then the water circulation in the pipes system is switched on at 8:20 in the morning. Figure 6.3 shows the hourly variation of the inlet and outlet water temperature during the day. The outlet temperature of the water ($T_{w,out}$) at 8:20 is almost 19 $^{\circ}$C and it reaches up to 42.5 $^{\circ}$C at 11:20, which is appropriate to run under floor heating system to supply heat to the room placed on the North side.

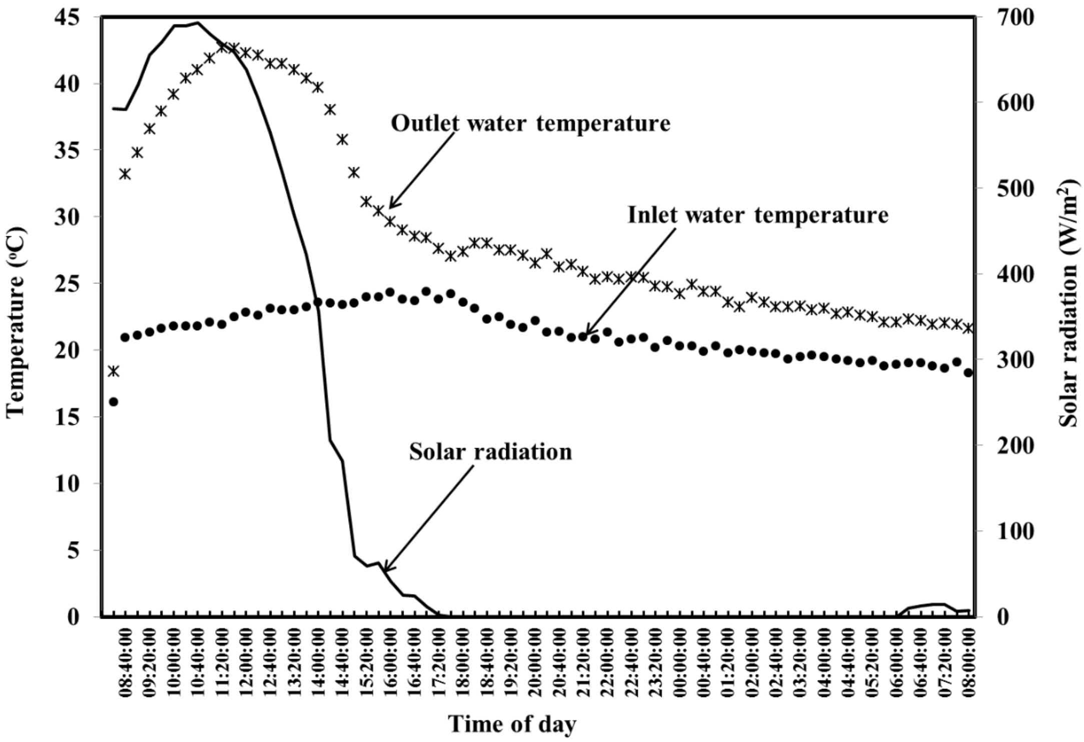

Figure 6.3. The inlet and outlet temperature of water on 10th March.

The temperature of the air gap between the TWS and the glass increases due to greenhouse effect which causes an increase in the temperature of the flowing water in the Pipe. In the present work an absorber plate is not used since it is required to heat the TWS as well. The inlet water temperature of the water ($T_{w,in}$) is approximately the same throughout the day.

Figure 6.4 is prepared for 11thMarch 2015, in which the weather is rainy and there was a week sunshine. The ambient temperature at 8:20 is approximately 15°C and at 15:40 it reaches approximately 16.7 °C. T_a is decreased to 11.6 °C on 12th March 2015 at 6:20 morning.

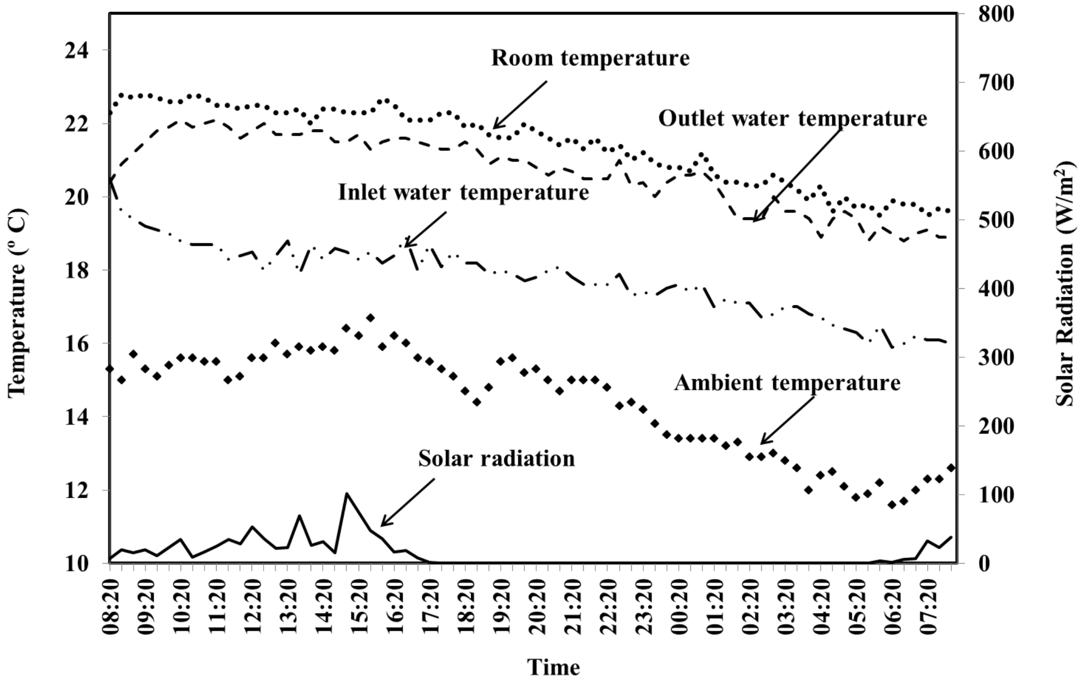

Figure 6.4. Solar radiation and temperatures on 11thMarch 2015 (rainy day).

On 11th March due to the cloudy weather the outer surface temperature of the wall is lower compared to the room and wall interior temperature is in the lowest temperature. The room temperature ranges is constantly ranges from 19.5 °C to 22.7 °C.

On 11th March all the thermocouples placed inside the wall and room indicates that the temperatures during 24 hours are approximately 23 °C and stable despite the absence of the sun. This is due to the full solar radiation received during 10th of March. Furthermore, the room and wall temperature on 11th March is adequate for a typical rainy day with solar radiation and ambient temperature being this level. Consequently, the result proves that the TSW is a heat storage masonry mass embedded in the building envelope in which heat is absorbed and stored and is used later , in the absence of the sun, when the heating is required.

It is evident from Figure 6.1 that the room temperature decreases quickly when the solar radiation vanishes from the surface of the wall. The reason of this problem is the lack of appropriate thermal insulation for Energy Laboratory that causes a great deal of heat loss. In addition, the heat flows to foundation base seen in Figure 6.5, causing the performance of the TWS to become less. Moreover, installation of typical glazing instead of double-glazing for existing windows and entrance can cause more heat loss. The TWS can be seen in Figure 6.5. During the construction of the TWS it is important to keep the foundation part as small as possible so that the heat is not lost to the foundation, but rather, stored in the wall for transmitting to the room at night time.

Figure 6.5. Foundation construction procedure of TSW

In order to investigate the effects of solar radiation and ambient temperature on the TSW a graph showing the performance in a 3-days row is prepared. The graph illustrates the outer and inner surface temperature of TSW and also, ambient and room temperature and solar radiation for three consecutive days which are initiated from 18th March and finished on 20the March 2015. The weather in these three selected days is different. On 18thMarch the weather is sunny and clear, while on 19th and 20th March the weather is cloudy-sunny and cloudy respectively.

The outer surface temperature of TSW is the highest temperature which is directly affected by the solar radiation. According to Figure 6.6, on 18th March the solar radiation is decreased at noon and the outer surface of the wall starts cooling at approximately 14:20. In addition the inner surface of TSW cooling period started one hour after that of the outer surface cooling period. This agrees well with Kalogirou's findings. The wall thickness they studied ranged from 0.15 m to 0.25 m. In addition, according to the Fuller Moore studies the delay in conducting heat with 0.16 m wall thickness through the TSW is around 6.8 hours, and also it is important to defer the maximum heating effects to the hours when the excessive heating is required. In this project, as it mentioned in chapter 3 the thickness of the TSW is 0.16 m which is amongst the suitable wall thickness ranges. Therefore, heat loses due to lack of suitable insulation and aforementioned problems are the cause of this problem.

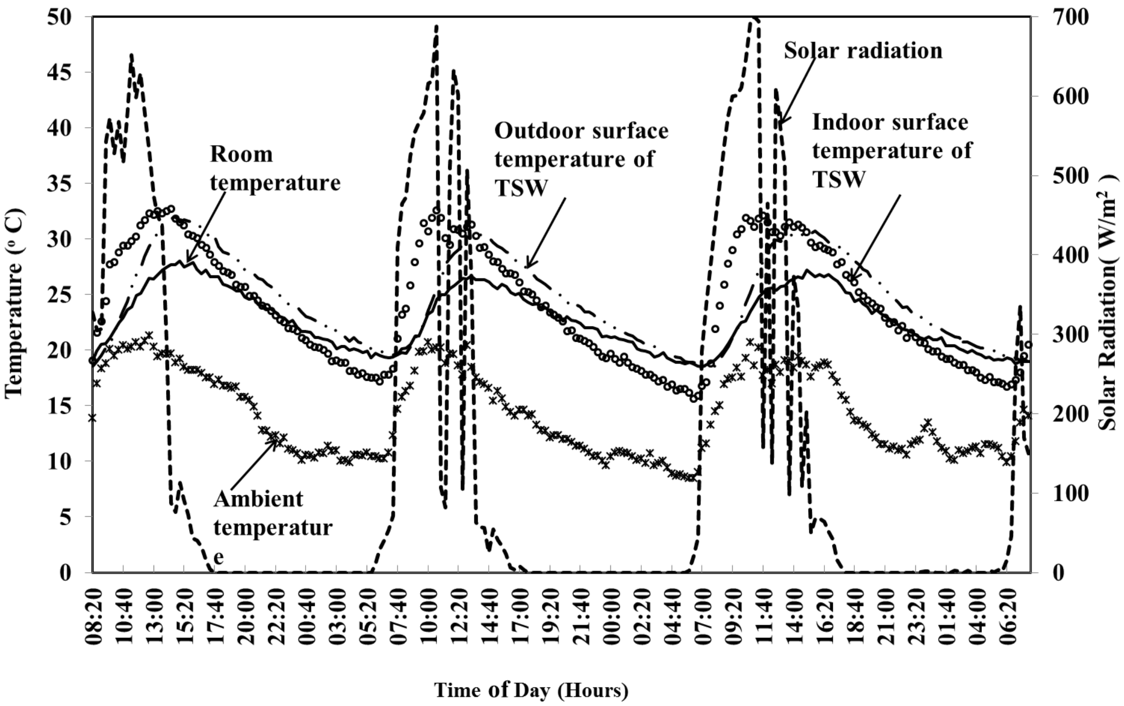

Figure 6.6. Inner and outer surface temperature of TSW and solar radiation between 18/03/2015 and 20/03/2015.

In Figure 6.6 the difference between T_r and T_a shows that TSWs can be appropriate for heating applications. For example on 18th March T_r reaches a maximum values of 25 °C at 15:00 while T_a is recorded to be 19.2 °C at the same hour. At night time T_a decreases considerably and at 7:00 o'clock in the morning it has a value of 10.8 °C, while at this time T_r is measured to be 19.3 °C providing a comfortable environment in the room.

On 19th and 20th March before noon the weather was sunny but in the afternoon it became cloudy. The existing solar radiation fluctuation in these days is due to the cloudy weather. It can be seen in Figure 6.7 that the inlet and outlet water temperatures to the solar collector display a favorable energy gain.

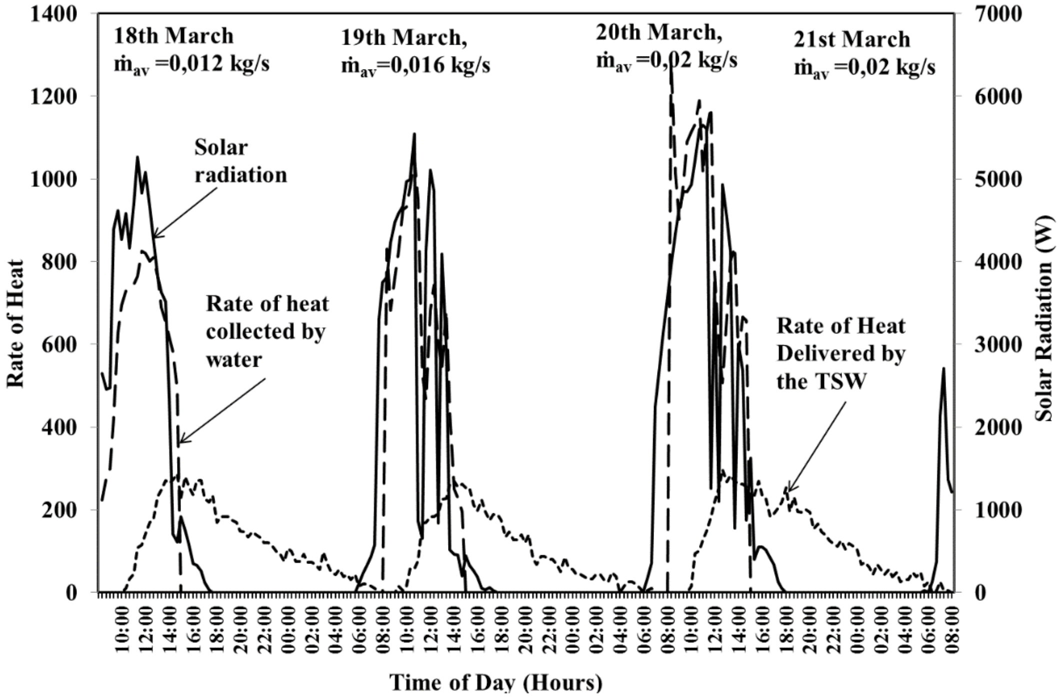

Figure 6.7. The inlet and the outlet temperature of the water pipes system.

On each day the pump is turned on at approximately 8:00 and the recordings started at 8:20. The pump was turned off at 15:00, although the recordings continued until 8:00 next day. The experiments were conducted with different mass flow rates: 0.012 kg/s, 0.016 kg/s and 0.02 kg/s for 18th, 19th and 20th of March respectively.

The temperature of the flowing water increases as the solar radiation increases. On 18th March the temperature of the water flowing of the solar collector reached 39 $^{\circ}$C and then it fell gradually to 29 $^{\circ}$C at 15:00 just before the pump is stopped.

With this temperature range it is possible to run under floor heating system to supply heat to the room which is placed on the North side, if enough volume of warm water is accumulated in the tank. Moreover, with installing thermal insulation for the water tank storage the heat losses throughout the tank decreases and the temperature of stored water in the tank remains more constant to domestic usage at night time.

Rate of heat delivered to the room, rate of heat collected by water copper pipes system and solar radiation are illustrated in Figure 6.8 for three consecutive days with different mass flow rates.

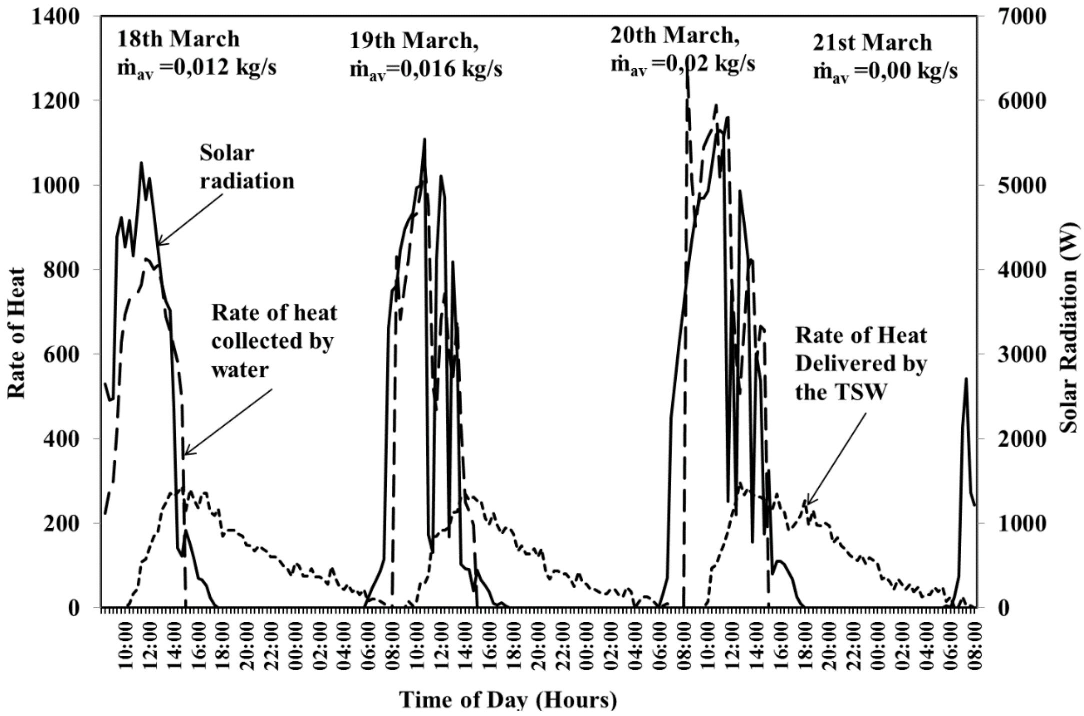

Figure 6.8. Hourly rate of heat delivered by TSW, collected by water and solar radiation for March 18, 19 and 20.

The heat gain by water (Q_w) reached a value of 800 W when the solar radiation (S) is 5262 W and then plunged to 612 W in two hours after noon as the solar radiation decreased to 700 W at 2:40. The reason of the sharp decrease of the rate of heat collected by water to zero is that the pump operation is stopped. In addition, the same condition in 18th March is accomplished for 19th and 20th March as well. The rate of heat collected by water is increased as the mass flow rate of water is increased in the last two consecutive days while the solar radiation is almost the same as the first day.

The rate of heat delivered by TSW (Q_{tw}) for one day is calculated as the total heat delivered by radiation and convection from the inner wall surface to the room. As it mentioned in chapter 2, TSWs are tardy in morning warm up, and also in this project TSW is unvented. Therefore it took time for the transferred heat to reach from outer wall surface to the inner wall surface. On 18th March the room warming up process is started at approximately 10:00, while the first sunshine on the outer wall surface is eradiated at approximately 5:00 in the morning. This issue is appeared on 19th and 20th March as well. Due to profitable sunshine in the morning on 19th March the morning warm up process is started earlier and around 9:00.

The area under the rate of heat graphs in Figure 6.9 show the heat energy collected by the pipes and that is supplied during three days to the room. The total heat energy achieved by the system is calculated as summation of rate of heat collected by water and the rate of heat delivered to the room.

Rate of heat collected by water, rate of heat delivered by TSW, room temperature and ambient temperature of three consecutive days are shown in Figure 6.9.

During the three consecutive days the room temperature swings between 28 °C and 18.8 °C range which is a comfortable range. In addition, in the coldest time on 19th March at 6:20 when the ambient temperature is decreased to 8.5 °C the room temperature is 18.8 °C, and the rate of heat delivered to room space is around 5 W. however, the rate of heat delivered increases during the day time. It reaches a value of 262 W at 14:20.

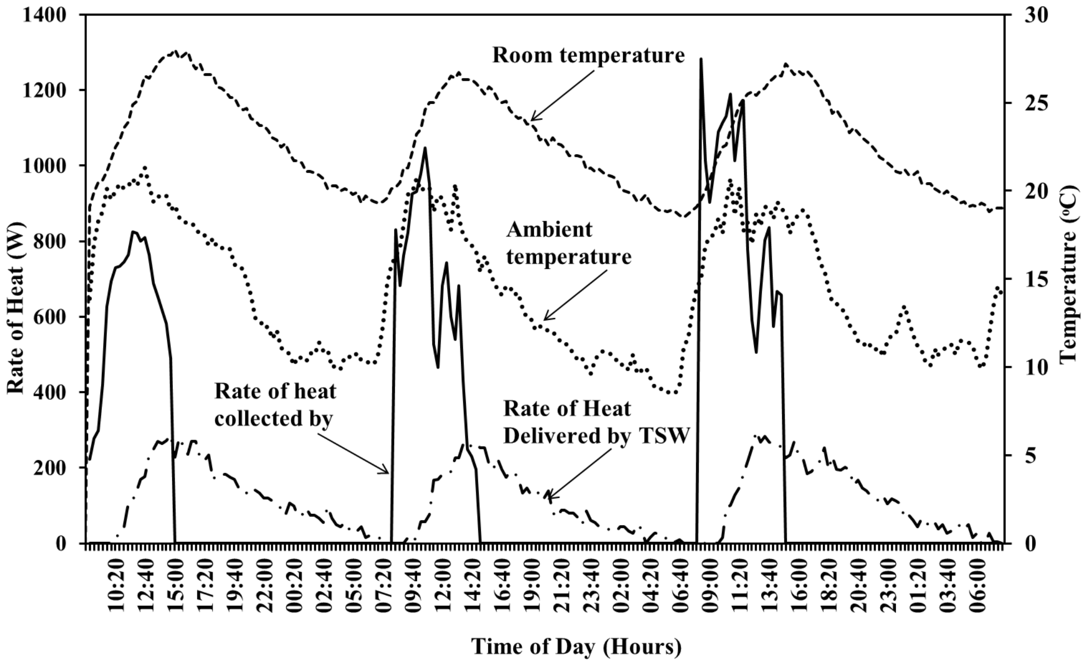

Figure 6.9. Hourly room gain, room and ambient temperature for March 18, 19 and 20.

Thermocouples location and temperature distribution at the interior surface of the TSW during 24 hours for three consecutive days are shown in Figure 6.10. The vertical axis shows the temperature and the horizontal axis illustrate the placement of the thermocouples inside the wall which are installed 4 cm apart from each other. The graphs on the left- hand side show the solar heating regime and the right- hand side shows the cooling regime.

On 18thMarch the solar heating process of the TSW is started at 7:20 morning and it is finished at 14:40. The outer surface temperature of the TSW is less than the other wall points before 8:20. Therefore, during this time the TSW is losing heat. With increasing in solar radiation and ambient temperature, the outer surface temperature of the wall is increased and became more than the other points. Parallel to the increasing in outer wall temperature, thermocouples placed in different interior points of the TSW illustrate that the temperature distribution inside the wall is increasing as well.

On 18th March the cooling period of TSW is started immediately after the sunshine disappeared from the TSW surface at 15:20. The cooling period graph of TSW illustrates that the temperature distribution inside the wall from point 4 to 12 is almost constant during this time. The outer surface temperature of TSW is lowest during cooling period.

All the aforementioned description for the TSW temperature distribution is expressible for 19thand 20th March, except that the cooling period for these two days is started one hour earlier at 13:20.

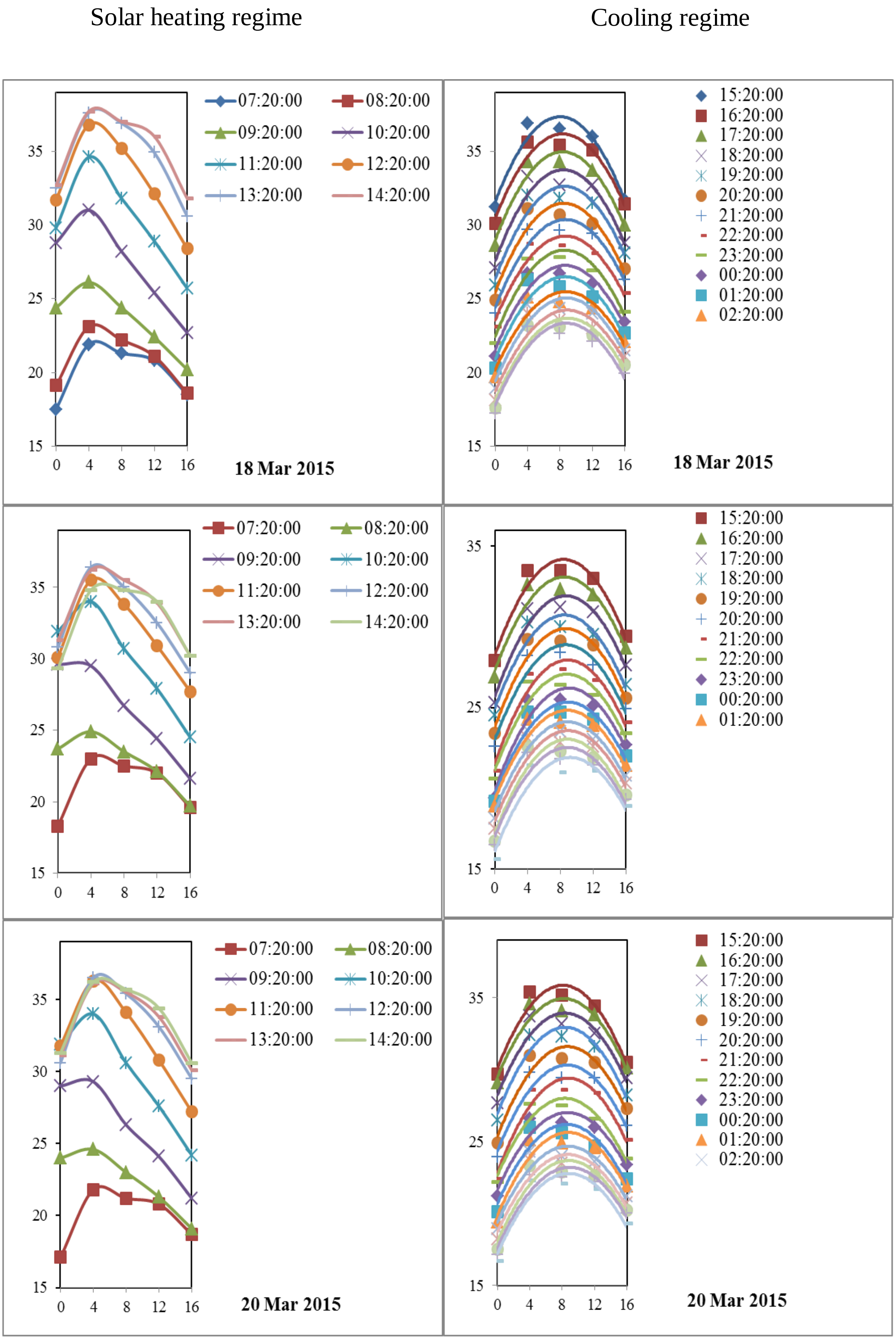

Figure 6.10. Temperature distribution inside the TSW

As it is mentioned in chapter 4, the efficiency of TSW is the total heat delivered by the TSW to the room divided by the total heat gained by solar radiation. It is noticeable that the heat transfer is assumed as one direction. In addition, the efficiency of hybrid TSW-water heating system is defined as the summation of the heat delivered by TSW to the room and heat collected by water copper pipes system over the total heat gained by solar radiation.

The total efficiency and TSW efficiency in some selected days with different weather condition is provided in Figure 6.11.

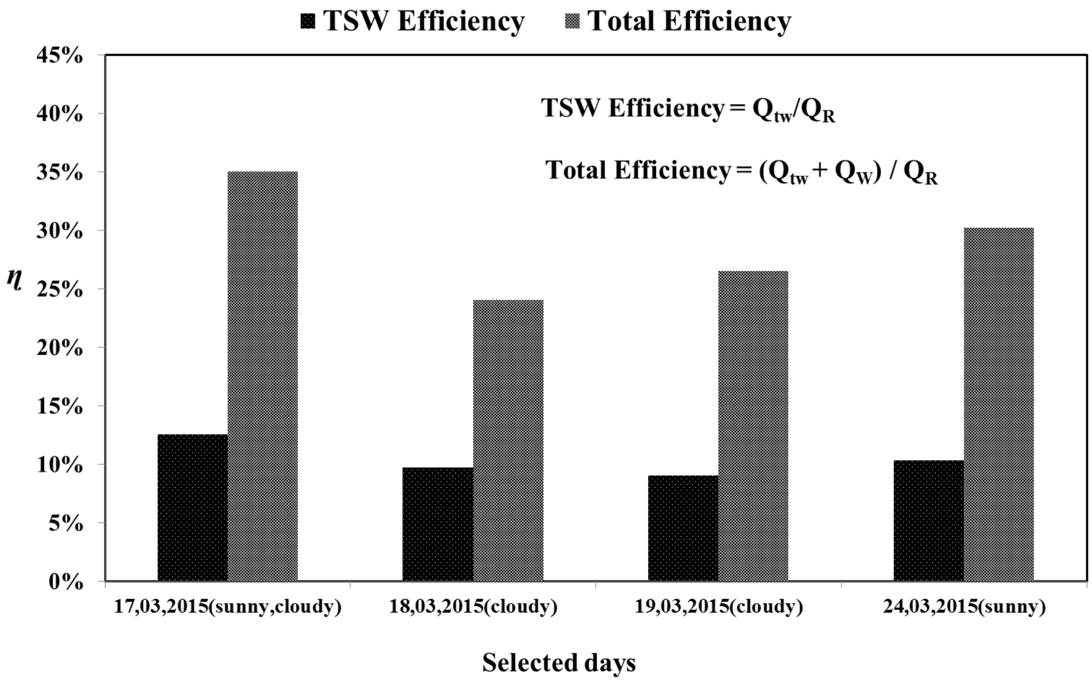

Figure 6.11. Total efficiency and TSW efficiency

The efficiency range of TSW is between 9% on 19th March with cloudy weather and 13% on 17th March with sunny weather. As expected, the efficiency of the TSW in sunny day is higher than the cloudy day.

The total efficiency with considering the collected heat by water copper pipes is approximately 35% in sunny day. The existing of water pipes system has a major designation in the hybrid TSW-water heating system efficiency. A comparison between the TSW efficiency and water copper pipes system efficiency is displayed in Figure 6.12.

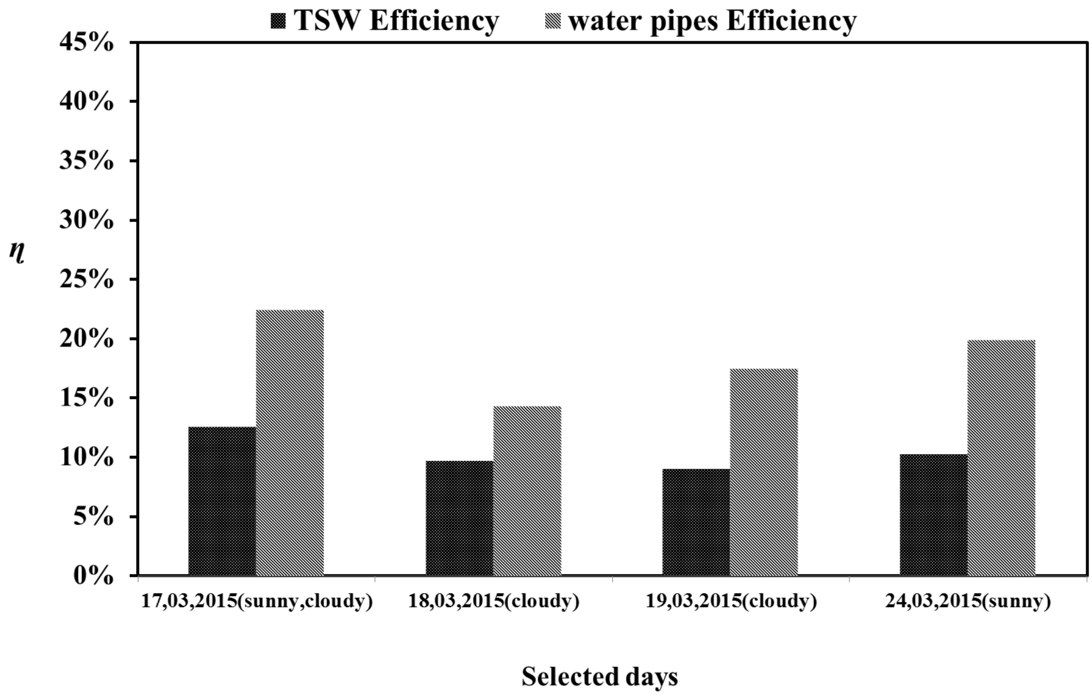

Figure 6.12. TSW and water copper pipes efficiency

Although the efficiency of the water pipes system is more than the TSW, but the performance of TSW system to supply heat at night time is impressive. In absence of sun during night time water pipes temperature is not profitable to supply heat to the room, but the TSW which is started cooling process is still supplying heat to the room.

It is noticeable that the existing water pipes system on the TSW surface has effect on TSW efficiency. Moreover, creating shadow by pipes on TSW surface might reduce the TSW efficiency and total efficiency. Unfortunately, due to lack of another energy laboratory with the similar TSW construction and facilities, recording data in the same day to investigate the effects of water pipes system on TSW performance is impossible.

Water collector efficiency versus time for three days with different climate is provided in Figure 6.13.

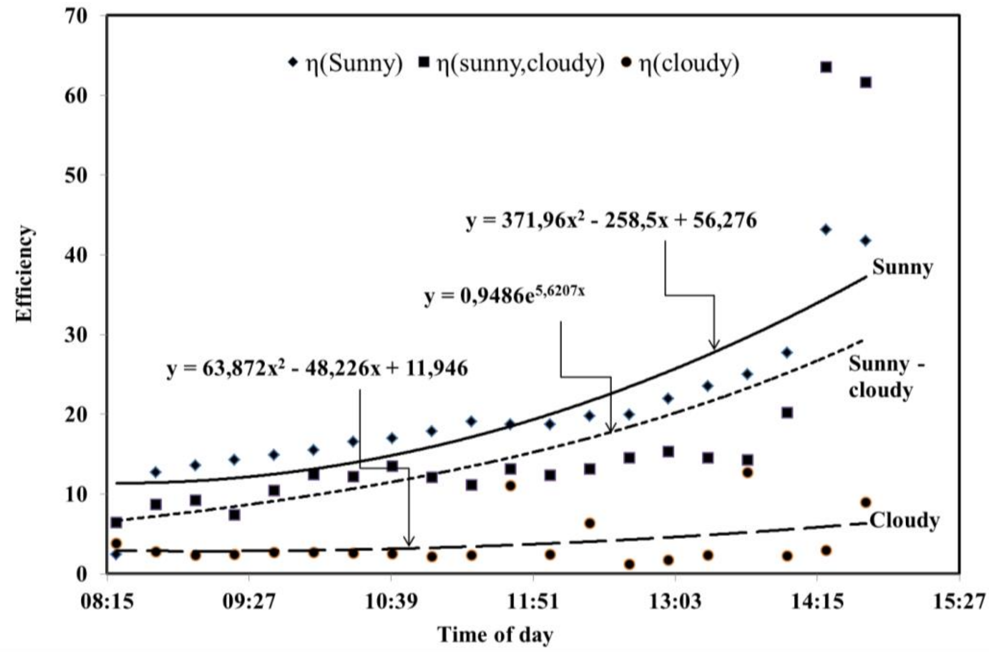

Figure 6.13. Variation of collector efficiency in different climates.

The thermal efficiency of water copper pipes system during the day is increased with increasing in solar radiation.

It is noticeable that between 2:20 and 2:40 in sunny and sunny-cloudy day, the efficiency rise sharply in the graph. The reason is the mistake in recording solar radiation intensity. One probability is when the pyranometer was recording the solar radiation intensity; cloud concealed the sun exactly at that time.

In chapter 5, errors and equations related to the experimental investigation were illustrated. The average values for temperature, solar radiation and mass flow rate are found 17.36 $^{\circ}$C, 591 W/m^2 and 0.02 kg/s, respectively on March 2015. The fractional uncertainty according to equation (12) for water collector and TSW efficiency is found to be 0.07 and 0.04, respectively.

Chapter 7

CONCLUSION AND FURTHER WORK

The aim of this study is to investigate the performance of the TSW of the Solar Energy Research, Inspection and Training (SolERIT) laboratory in the Eastern Mediterranean University. Solar radiation and temperatures of the ambient, the wall, the indoors, the water inlet and outlet of the collector were monitored and recorded on selected days of March.

It is discovered that when a TSW is coupled with a water heating system by means of fastening an array of pipes on the wall would deliver satisfactory performance for winter heating purposes. The performance of the TSW would not be significantly affected by the existence of the pipes, while on the other hand it was shown that it can be possible to have solar heating alternatives for other rooms of any building not facing to southern direction.

On the 17th March there was a clear day with the solar intensity reaching 677 W/m^2. The efficiency of the TSW and the collector together was estimated to be 35% while the efficiency of TSW without the water collector was approximately 12%. The existence of water pipes system has a major effect in the efficiency of the hybrid TSW-water heating system.

It is observed that the water collector improves the performance of the hybrid TSW-water heating system and low-grade heat can be accumulated in a tank for utilizing in other heating applications. As a result, installing water pipes on the TSW has profitable benefits

It was observed that the room temperature had a 9-10 ^{o}C swing between days and nights. This is because the TSW was oversized for the room which did not have thermal insulation leading to relatively higher heat losses at night times. It is important to use thermal insulation on the building envelope and repeat the experiments in the future in order to see how much difference it makes.

The solar heat collection of the water passing through the pipes could be enhanced by adding absorber plates in the form of fins. An experiment can be performed as a future work. It would be interesting to find out if there is an improvement on the solar collector and how much compromise on the performance of the TSW is made.

REFERENCES

[1] Wang, F., Manzanares-Bennett, A., Tucker, J., Roaf, S., & Heath, N. (2012). A feasibility study on solar-wall systems for domestic heating – An affordable solution for fuel poverty. *Solar Energy*. 86, 2405-2415.

[2] Moore, F. (2010). Environmental Control Systems: Heating, Cooling, Lighting, illustrated. McGraw-Hill.

[3] Albanese, M. V., Robinson, B. S., Brehob, E. G., & Sharp M. K. (2012). Simulated and experimental performance of a heat pipe assisted solar wall. *Solar Energy*. 86, 1552-1562.

[4] Jaber, S,. & Ajib, S. (2011). Optimum design of Trombe wall system in mediterranean region. *Solar Energy*. 85, 1891-1898.

[5] Kalogirou, S. A., Florides, G., & Tassou, S. (2002). Energy analysis of buildings employing thermal mass in Cyprus. *Renewable Energy*. 27, 353-368.

[6] Jie, J., Bin, J., Hua, Y., Tin-tai, C., Wei, H., & Gang, P. (2008). An experimental and mathematical study of efforts of a novel photovoltaic-Trombe wall on a test room. *Internatiomal Journal of Energy Research*. 32, 531-542.

[7] Bellamy, L. A. (2012). An Experimental Assessment of the Energy Performance of Novel Concrete Walls Embedded with Mini Solar Collectors. *Energy Procedia*. 30, 29-34.

[8] Kara, Y. A., & Kurnuç, A. (2012). Performance of coupled novel triple glass and phase change material wall in the heating season: An experimental study. *Solar Energy*. 86, 2432-2442.

[9] Smolec, W., & Thomas, A. (1993). Theoretical and experimental investigations of heat transfer in a trombe wall. *Energy Conversion and Management*. 34, 385-400.

[10] Robinson, B. S., Chmielewski, N. E., Knox-Kelecy, A., Brehob, E. G., & Sharp, M. K. (2013). Heating season performance of a full-scale heat pipe assisted solar wall. *Solar Energy*. 87, 76-83.

[11] Briga-Sá, A., Martins, A., Boaventura-Cunha, J., Lanzinha, J. C., & Paiva, A. (2014). Energy performance of Trombe walls: Adaptation of ISO 13790:2008(E) to the Portuguese reality. *Energy and Buildings*. 74, 111-119.

[12] Yilmaz, Z., & Basak Kundakci, A. (2008). An approach for energy conscious renovation of residential buildings in Istanbul by Trombe wall system. *Building and Environment*. 43, 508-517.

[13] Saadatian, O., Sopian, K., Lim, C. H., Asim, N., & Sulaiman, M. Y. (2012). Trombe walls: A review of opportunities and challenges in research and development. *Renewable and Sustainable Energy Reviews*. 16, 6340-6351.

[14] Eshraghi, J., Narjabadifam, N., Mirkhani, N., Sadoughi, K. S., & Ashjaee, M. (2014). A comprehensive feasibility study of applying solar energy to design a zero energy building for a typical home in Tehran. *Energy and Buildings*. 72, 329-339.

[15] Atikol, U., Aldabbagh, L. B. Y., & Sezai, I. (2006). Effect of standing time after usage on the performance of storage-type domestic electrical water-heaters. *Journal of the Energy Institute*. 79, 53-58.

[16] Cengel, Y. (2006). *Heat and Mass Transfer: A Practical Approach*: McGraw-Hill.

[17] Holman, J. P. (2001). *Experimental Methods for Engineers*: McGraw-Hill.

[18] El-Khawajaha, M. F., Egelioglub, F., & Ghazalb M. (2014). Finned Single-pass Solar Air Heaters with Wire Mesh as an Absorber Plate. *Green Energy*. 12, 108-116.

APPENDICES

Appendix A: MATLAB program for evaluating the k-value (Thermal Conductivity)

```
>> T1=15;
>> T2=20;
>> T3=25;
>> T4=30;
>> T5=35;
>> K1=0.02476;
>> K2=0.02514;
>> K3=0.02551;
>> K4=0.02588;
>> K5=0.02625;
>> t=[...];
>> for ti=t
if (ti>T1 & ti<T2)
K=K1+(((K2-K1)/(T2-T1))*(T2-ti));
elseif (ti>T2 & ti<T3)
K=K2+(((K3-K2)/(T3-T2))*(T3-ti));
elseif (ti>T3 & ti<T4)
K=K3+(((K4-K3)/(T4-T3))*(T4-ti));
else (ti>T4 & ti<T5)
K=K4+(((K5-K4)/(T5-T4))*(T5-ti));
end;
disp( [K] )
end;
```

Appendix B: MATLAB program for evaluating the Pr-value (Prandtl Number)

```
>> T1=15;
>> T2=20;
>> T3=25;
>> T4=30;
>> T5=35;
>> K1=0.7323;
>> K2=0.7309;
>> K3=0.7296;
>> K4=0.7282;
>> K5=0.7268;
>> t=[…];
>> for ti=t
if (ti>T1 & ti<T2)
K=(K2+(((K1-K2)/(T2-T1))*(T2-ti)));
elseif (ti>T2 & ti<T3)
K=(K3+(((K2-K3)/(T3-T2))*(T3-ti)));
elseif (ti>T3 & ti<T4)
K=(K4+(((K3-K4)/(T4-T3))*(T4-ti)));
else (ti>T4 & ti<T5)
K=(K5+(((K4-K5)/(T5-T4))*(T5-ti)));
end;
disp( [K] )
end;
```

Appendix C: MATLAB program for evaluating the ν-value (Dynamic Viscosity)

```
>> T1=15;
>> T2=20;
>> T3=25;
>> T4=30;
>> T5=35;
>> K1=(1.470*(10^-5));
>> K2=(1.516*(10^-5));
>> K3=(1.562*(10^-5));
>> K4=(1.608*(10^-5));
>> K5=(1.655*(10^-5));
>> t=[…];
>> for ti=t
if (ti>T1 & ti<T2)
K=K1+(((K2-K1)/(T2-T1))*(T2-ti));
elseif (ti>T2 & ti<T3)
K=K2+(((K3-K2)/(T3-T2))*(T3-ti));
elseif (ti>T3 & ti<T4)
K=K3+(((K4-K3)/(T4-T3))*(T4-ti));
else (ti>T4 & ti<T5)
K=K4+(((K5-K4)/(T5-T4))*(T5-ti));
end;
disp( [K] )
end;
```